

1st GEOCHRONOLOGY AND MASS SPECTROMETRY WORKSHOP-2022



EBOOK ISBN : 978-605-74442-7-1

GEOMSWHSP

Konya/TURKEY

12-13 May 2022

**12-13 MAY 2022 - KONYA TECHNICAL UNIVERSITY,
GEOLOGICAL ENGINEERING DEPARTMENT**

Geochronology and Mass Spectrometry Workshop

📍 **Location:** - Konya Technical University, Geological Engineering
Department, TURKEY

ABSTRACTS AND PROCEEDINGS BOOK



EBOOK ISBN : 978-605-74442-7-1

T.C.

Kültür ve Turizm Bakanlığı

Matbaa Sertifika No: 46389

Chairmen: Prof. Dr. Fetullah ARIK & Prof. Dr. Kürşad ASAN

Honorary speaker: Prof. Dr. Axel K. SCHMITT

Convenor: Dr. Gülin GENÇOĞLU KORKMAZ

Editor: Dr. Gülin GENÇOĞLU KORKMAZ (Geological Engineering Department -Konya Technical University)

Location: Konya Technical University, Geological Engineering Department, Konya/TURKEY (12-13 May 2022)

**1st GEOCHRONOLOGY AND MASS SPECTROMETRY
WORKSHOP 2022**

**12-13 May 2022 by the Konya Technical University,
Geological Engineering Department**

<https://geomswshp.sub.fyi/>

**ABSTRACTS AND
PROCEEDINGS BOOK**



EBOOK ISBN : 978-605-74442-7-1
T.C.

Kültür ve Turizm Bakanlığı
Matbaa Sertifika No: 46389

E-mail:

gencoglukorkmaz@gmail.com

Address:

Konya Technical University, Geological Engineering Department, Konya/TURKEY

More info is available on the web page:

<https://geomswshp.sub.fyi/>

DISCLAIMER

This book contains **abstracts and proceedings** approved by the 1st GEOCHRONOLOGY AND MASS SPECTROMETRY WORKSHOP 2022 Scientific Committee. The authors are responsible for the content of the abstracts and conference proceedings (title, names, name order, figures, tables, addresses, references) and accuracy of given information in their works. The publishers (or editors) make no representation, express or implied, with regard to the accuracy of the information contained in this book and cannot accept any legal responsibility for any errors or omissions or ethical problem that may be made. No part of this book may be reproduced or transmitted in any form or by any means, electronic or mechanical, for any purpose, without the express written permission of the authors, without the written permission of the publisher. All rights reserved.

Invitation

As the organizing committee, we are honored to invite you to attend **1st GEOCHRONOLOGY AND MASS SPECTROMETRY WORKSHOP 2022** which will be held online on 12-13 May 2022 by the Konya Technical University, Geological Engineering Department. This workshop will be useful for scientists, students, and researchers who are interested in studies such as the events from the formation of the universe to the present, the dating of the magmatism and volcanic activities, time scales of magmatic processes, the effect of humanity and volcanism, and the revealing of the magmatism-tectonism relationship. In this workshop, the methods used for geochronological studies and case studies will be explained and discussed.

Through the workshop, it will be possible to establish new partnerships, to share knowledge and experiences.

The purpose of the workshop is to give information about geological, petrological, and geochronological information to participants. Also, this workshop aims to provide connections for students and young researchers, and also to provide opportunities for experts to share and discuss their experiences.

Chairman
Prof. Dr. Kürşad ASAN

COMMITTEES

HONORARY COMMITTEE

Prof. Dr. Axel K. Schmitt, Heidelberg University, Institute of Earth Sciences

Prof. Dr. Yusuf Kağan Kadioğlu, Ankara University, Department of Geological Engineering

Prof. Dr. Gonca Gençalioğlu Kuşcu, Muğla Sıtkı Koçman University, Department of Geological Engineering

Prof. Dr. Hamdi Şükür Kılıç, Selçuk University, Physics Department (Advanced Technologies Research and Application Center Laser Laboratory)

Assoc. Prof. Dr. Eren Şahiner, Ankara University, Nuclear Sciences Institute

Assoc. Prof. Dr. Ersin Koralay, Dokuz Eylül University, Department of Geological Engineering

Assoc. Prof. Dr. Fatih Karaoglan, Cukurova University, Department of Geological Engineering

Assoc. Prof. Dr. Altuğ Hasözbeş, Laboratorio De Series De Uranio/Centro Nacional de Investigación sobre la Evolución Humana, Cenieh/Spain

Assist. Prof. Dr. Kiymet Deniz, Ankara University

Dr. Gönenç Göçmengil, İstanbul Metropolitan Municipality

ORGANIZING COMMITTEE

HONORARY CHAIR

Prof. Dr. Babür ÖZÇELİK (RECTOR, Konya Technical University)

CHAIRMEN

Prof. Dr. Fetullah ARIK (Head of Geological Engineering Department, Konya Technical University)

Prof. Dr. Kürşad ASAN (Konya Technical University)

CONVENOR

Dr. Gülin GENÇOĞLU KORKMAZ (Konya Technical University)

ADVISORY BOARD

Prof. Dr. Nilgün Güleç (Middle East Technical University)

Prof. Dr. Yusuf Kağan Kadioğlu (Ankara University)

Prof. Dr. Halim Mutlu (Ankara University)

Prof. Dr. Erkan Aydar (Hacettepe University)

Prof. Dr. Hüseyin Kurt (Konya Technical University)

Prof. Dr. Kürşad Asan (Konya Technical University)

Prof. Dr. Tamer Koralay (Pamukkale University)

Prof. Dr. Emrah Yalçın Ersoy (Dokuz Eylül University)

Prof. Dr. Cüneyt Akal (Dokuz Eylül University)

Assist. Prof. Dr. Bahattin Güllü (Aksaray University)

MEMBERS

Assist. Prof. Dr. Kiymet Deniz (Ankara University)

Assist. Prof. Dr. Yasemin Gündoğdu (Selçuk University)

Assist. Prof. Dr. Hatice Ünal Ercan (Konya Technical University)

Assist. Prof. Dr. Fatma Gülmez (İstanbul Technical University)

Dr. Gönenç Göçmengil (The İstanbul Metropolitan Municipality)

Dr. Gülin Gençoğlu Korkmaz (Konya Technical University)

Dr. Yeşim Özgen (Konya Technical University)

Dr. Ali Bozdağ (Konya Technical University)

Dr. Mehmet Yavuz Hüseyinca (Konya Technical University)

Dr. Zeynep Cansu Ayturan (Konya Technical University)

MSc. Yasin Akin Ayturan (KTO Karatay University)

MSc. Mesut Gündüz (Konya Technical University)

EDITORIAL BOARD

Dr. Gülin Gençoğlu Korkmaz (Geological Engineering Department -Konya Technical University)

SUPPORTING ORGANIZATIONS

Konya Technical University

Chamber of Geological Engineers

Ankara University Geosciences Application and Research Center (YEBİM)

SCIENTIFIC BOARD

Prof. Dr. Axel K. Schmitt, Heidelberg University, Institute of Earth Sciences

Prof. Dr. Yusuf Kağan Kadioğlu, Ankara University, Geological Engineering

Prof. Dr. Erkan Aydar, Hacettepe University, Geological Engineering

Prof. Dr. Halim Mutlu, Ankara University, Geological Engineering

Prof. Dr. Nizamettin Kazancı, Ankara University, Geological Engineering

Prof. Dr. Tamer Koralay, Pamukkale University, Geological Engineering

Prof. Dr. Mehmet Arslan, Karadeniz Technical University, Geological Engineering

Prof. Dr. İrfan Temizel, Karadeniz Technical University, Geological Engineering

Prof. Dr. Yener Eyüboğlu, Karadeniz Technical University, Geological Engineering

Prof. Dr. Hüseyin Kurt, Konya Technical University, Geological Engineering

Prof. Dr. Kürşad Asan, Konya Technical University, Geological Engineering

Prof. Dr. Fetullah Arik, Konya Technical University, Geological Engineering

Prof. Dr. Kerim Koçak, Konya Technical University, Geological Engineering

Prof. Dr. Hamdi Şükür Kılıç, Selçuk University, Department of Physics-and-Advanced Technologies Research and Application Center

Prof. Dr. Nilgün Güleç, Middle East Technical University, Geological Engineering

Prof. Dr. Gonca Gençalioğlu Kuşcu, Muğla Sıtkı Koçman University, Geological Engineering

Prof. Dr. İlkay Kuşcu, Muğla Sıtkı Koçman University, Geological Engineering

Prof. Dr. Emrah Yalcın Ersoy, Dokuz Eylül University, Geological Engineering

Prof. Dr. Cüneyt Akal, Dokuz Eylül University, Geological Engineering

Assoc. Prof. Dr. Ersin Koralay, Dokuz Eylül University, Geological Engineering

Assoc. Prof. Dr. Eren Şahiner, Ankara University, Nuclear Sciences Institute

Assoc. Prof. Dr. Fatih Karaoglan, Çukurova University, Geological Engineering

Assist. Prof. Dr. Bahattin Güllü, Aksaray University, Geological Engineering

Assist. Prof. Dr. Kiymet Deniz, Ankara University, Geological Engineering

Assist. Prof. Dr. Yasemin Gündoğdu, Selçuk University, Department of Physics-and- Advanced Technologies Research and Application Center

Assist. Prof. Dr. Serap Yiğit Gezgin, Selçuk University, Department of Physics-and-Advanced Technologies Research and Application Center

Assist. Prof. Dr. Gürsel Kansun, Konya Technical University, Geological Engineering

Assist. Prof. Dr. Hatice Ünal Ercan, Konya Technical University, Geological Engineering

Assist. Prof. Dr. Fatma Gülmmez, İstanbul Technical University, Geological Engineering

Dr. Yeşim Özen, Konya Technical University, Geological Engineering

Dr. Gülin Gençoğlu Korkmaz, Konya Technical University, Geological Engineering

Dr. Ece Kirat, University of Exeter, Camborne School of Mines, Geological Engineering

Dr. Gönenç Göçmengil, The İstanbul Metropolitan Municipality, Geological Engineering

INVITED SPEAKERS



SCIENTIFIC PROGRAM

Workshop with international participation

GEOCHRONOLOGY AND MASS SPECTROMETRY

WORKSHOP (GEOMSWSHP2022 12-13 May 2022)

<https://geomswshp.sub.fyi/>

Konya Technical University, Geological Engineering Department

SCIENTIFIC PROGRAM

Thursday, MAY 12, 2022

Konya Technical University, Engineering Faculty Meeting Hall-2 (Online)

09:30-10:00	Opening Ceremony Chair person: Dr. Gülin Gençoğlu Korkmaz
10:00 - 11:15	“Silisik Magmalarda Zirkon Kristalleşme Koşulları ve Jeokronoloji için Önemleri” "Conditions of Zircon Crystallization in Silicic Magmas and Implications for Geochronology" Prof. Dr. Axel K. Schmitt Heidelberg University Institute of Earth Sciences
11:15-12:15	“Felsik ve Mafik Kayalarda Yaşılandırma ve Karşılaılan Sorunlar: Jeokronolojide Doğru Mineral Seçimi Nasıl Olmalı?” "Dating of the Felsic and Mafic Rocks and Encountered Problems: How to Choose the Right Mineral in Geochronology?" Prof. Dr. Yusuf Kağan Kadıoğlu Ankara University, Geological Engineering Department
12:15 – 13:30	Lunch Break Chair person: Dr. Yeşim Özen
13:30 - 14:30	"Yakındaki Probleme Uzaktan Bir Çözüm: Datça Yarımadasında (Muğla) Depolanan İncirli-Kyra Distal Tefrasının Çoklu Teknik Jeokronolojisi" "A Distal Solution to a Proximal Problem: Multi-technique Geochronology of Distal Nisyros-Kyra Tephra on Datça Peninsula (Muğla)" Prof. Dr. Gonca Gençaloğlu Kuscu, Muğla Sıtkı Koçman University Geological Engineering
14:30 – 15:30	“Menderes Masifi'ndeki Jeolojik Problemlerin Çözüme Zirkon U-Pb Yaşı Tayini İle Yaklaşımı” "Zircon U-Pb Dating Methods for the Solution of Geological Problems in the Menderes Massif" Assoc. Prof. Dr. Ersin Koralay Dokuz Eylül University, Geological Engineering
15:30-15:40	Break Chair person: Dr. Gönenç Göçmengil
15:40 - 16:40	“Düşük Sıcaklık Termokronolojisi ve Jeolojide Kullanımı” "Low Temperature Thermochronology and Its Usage in Geology" Assoc. Prof. Dr. Fatih Karaoglan Çukurova University, Geological Engineering
16:40-17:40	“Lazer Ablasyon Tekniği ve Bazı Jeolojik Uygulamalar” "Lasers Ablation Technique and Some Geological Applications" Prof. Dr. Hamdi Şükür Küçük Selcuk University Physics Department
Friday, MAY 13, 2022	
Konya Technical University, Engineering Faculty Meeting Hall-2 (Online)	
10:00 – 11:00	Chair person: Dr. Hatiye Ünal Ercan “Elektron Mikroprob ile Yaşılandırma Tekniği” "Dating Methods by using Electron Microprobe" Assist. Prof. Dr. Kiymet Deniz Ankara University, Geological Engineering Department
11:00–12:00	“Kuvaterner Jeokronolojisinde U-Th Yaşılandırma ve Uygulamaları” "U-Th Dating and its Applications in Quaternary Geochronology" Assoc. Prof. Dr. Altug Hasözbeck Laboratorio De Series De Uranio/Centro Nacional de Investigación sobre la Evolución Humana, Cemech/Spain
12:00-13:30	Lunch Break Chair person: Assist Prof. Dr. Fatma Gülmez
13:30 – 14:30	“Lüminesans tarihleştirmeye: Jeokronoloji çalışmalarındaki yeri ve geleceği” "Luminescence dating: its place and future in geochronological studies" Assoc. Prof. Dr. Eren Şahiner Ankara University, Institute of Nuclear Sciences
14:30-15:30	“LA-ICP-MS ile U-Pb Karbonat yaşılandırma uygulamaları” "U-Pb Carbonate dating applications with LA-ICP-MS" Dr. Gönenç Göçmengil İstanbul Metropolitan Municipality
15:30-16:15	“Karapınar Karacadağ Volkanitlerine Ait İlk U-Pb Zirkon Jeokronoloji Verileri ve Bölgenin Volcanostratigrafik Evrimi” "First U-Pb Zircon Geochronology Data of Karapınar Karacadağ Volcanics and Volcanostratigraphic Evolution of the Region" Dr. Gülin Gençoğlu Korkmaz Konya Technical University
16:15	Closing

12-13 Mayıs 2022 tarihleri arası wokshop bağlantı linki: https://teams.microsoft.com/l/meetup-join/19%3ameeting_NzdjZjAwYjQtNGI5Ny00NmUxLTkzZWltMDA1ZWjYjIIZjYz%40treadyv2/0?context=%7b%22Tid%22%3a%22af9a1a40-e030-4a92-a04f-902360660ce0%22%2c%22Oid%22%3a%220f407220-5e55-4a6b-b2f3-586f9a56536b%22%7d

GEOCHRONOLOGY

Geochronology is the science of detecting the age of rocks, fossils, and sediments using signatures inherent in the rocks themselves. Absolute geochronology can be accomplished through radioactive isotopes, whereas relative geochronology is provided by tools such as paleomagnetism and stable isotope ratios. K-Ar, Ar-Ar, Rb-Sr, Sm-Nd, U-Th-Pb, and fission track dating methods could be used for detecting the age of the effusive rocks. These methods can be used together or alone on minerals or whole rock. By using these methods we can detect the crystallization and/or the cooling ages of the intrusion and magmatism. The method and analytical technique (SIMS: Secondary Ion Mass Spectrometry; (U-Th)/He dating (Quadrupole Isotope-dilution Mass Spectrometry (MS-for He) and Inductively Coupled Plasma Mass Spectrometry (ICP-MS-For U and Th); LA-ICP-MS: Laser Ablation Inductively Coupled Plasma Mass Spectrometry); SHRIMP: Sensitive High-Resolution Ion Microprobe, etc.) to be used are determined by the mineralogical and chemical composition and/or petrographic properties of the rock.

Many dating methods such as U-Pb, U-Th/He, K-Ar (Ar-Ar), radiocarbon (14C), fission-track, and luminescence method could be applied on Quaternary aged volcanites (Danisik et al., 2017). U-Pb series methods and the usage of the robust minerals both physically and chemically (apatite, rutile, zircon) for the dating give more accurate results. Moreover, they can give information about the magma dynamics. Combination of zircon ages with geochemical indicators, for magmatic temperatures (Ti-in zircon content) and compositions (Zr / Hf, Eu / Eu, in zircon; La / Nd, Mg / Mn ratios in allanite) can provide information regarding dynamics of the evolution of the magmatic system (Schmitt, 2011).

Conditions of zircon crystallization in silicic magmas and implications for geochronology

Axel K. Schmitt

Department of Earth Sciences, Heidelberg University, Germany

Zircon is a key mineral for geological timekeeping from the Hadean to the Holocene. This is due to its ubiquitous occurrence in mostly felsic igneous, metamorphic, and sedimentary rocks, and the robustness of the U-Th-Pb decay system. When dating zircon, precise timing of a geological event such as tephra deposition or pluton intrusion is desired, but with increasing analytical precision and sensitivity, zircon data often spread beyond analytical uncertainty, resulting in a zircon age spectrum for a given rock sample. This behavior is distinct from age spread caused by Pb-loss affecting radiation-damaged zircon, as it demonstrably occurs for U-Pb ages of young zircon at inconspicuous U abundances, and for U-Th ages <300 ka where radioactive parents and daughters are extremely immobile. Instead, true zircon age spectra result from protracted zircon formation in a magmatic environment, and with sufficient data on zircon ages and formation conditions, they can reveal unique insights into processes within magma reservoirs.

Zircon saturates in silicic melts as a function of temperature, Zr-abundance, and melt chemistry that is typically expressed by a parameterization relating network-forming components such as Si and Al to network-modifiers such as Na, K, and Ca (e.g., Boehnke et al., 2013). Saturation concentrations typically decrease exponentially with temperature, so that high-temperature (early crystallized) zircon should predominate over low-temperature (late crystallized) zircon if a single batch of magma cools and crystallizes (Harrison et al., 2007). However, the cumulative mass distribution of zircon in a subvolcanic intrusive complex where a melt-bearing reservoir is sustained by influx of hot, mafic magma recharge, will be dominated by young zircon due to growth of the intrusion volume where zircon is saturated, and where the early-formed zircon population will become progressively diluted by younger zircon (e.g., Tierney et al., 2016; Weber et al., 2018). Sensitivity tests for different intrusive model geometries comprising (1) inflation of a magma reservoir due to recharge into the hot core of the intrusion vs. (2) downward vertical stacking of sills indicate that the duration of zircon crystallization is within a factor of two for both models at a prescribed recharge flux and geothermal gradient, thus permitting quantitative assessments of magma fluxes and volumes from zircon age spectra. Zircon crystallization age spectra and chemical compositions were obtained for late Pleistocene–Holocene volcanic rocks of Hasan Dağı and Erciyes Dağı, two neighboring (within

~120 km) large stratovolcanoes in central Anatolia with edifice volumes of 130–180 and ~300 km³, respectively (Friedrichs et al., 2021). Zircon extraction and analytical procedures were identical for both sets of samples: zircon rim analysis (U-Th geochronology and trace elements by secondary ionization mass spectrometry, SIMS) was followed by sectioning of the crystals to expose their interiors, which were again dated and their trace element compositions determined. Resulting zircon age spectra are continuously populated over the past ~300 ka in both cases, but with clear distinctions: Hasan Dağı zircon nucleated and crystallized steadily, whereas Erciyes Dağı zircon interior ages peak at ca. 100 ka, followed by a lull in zircon nucleation until it resumes at ca. 20 ka (Friedrichs et al., 2021). This lull correlates with an interval of eruptive inactivity and is also characterized by low Ti-in-zircon temperatures (~700 °C) and evolved compositions of zircon rims, whereas Hasan Dağı zircon rims and interiors are thermally and compositionally invariant (Ti-in-zircon average temperature ~750 °C). Modelling of zircon age spectra match these data for a steady or slightly decreasing recharge flux of 0.5 km³/ka for Hasan Dağı, whereas the ca. 100 ka peak in zircon nucleation followed by a nearly complete hiatus requires a low background recharge flux of 0.08 km³/ka that only spiked briefly at c. 100 and 20 ka (Friedrichs et al., 2021). Zircon age spectra thus reveal a thermally stable magma reservoir underneath Hasan Dağı, whereas melt-bearing volumes at Erciyes Dağı are likely small, isolated, and relatively cool. This is reinforced by comparatively high-temperature (820–1020 °C based on Fe-Ti oxide thermometry) eruptions of intermediate magma at Hasan Dağı with evidence for magma mingling, whereas recent Erciyes Dağı dome eruptions produced explosive rhyolites at comparatively low temperatures (780–870 °C; Friedrichs et al., 2021). Geophysical evidence for a low resistivity anomaly at 4–6 km depth further supports a sizable and long-lived magma reservoir underneath Hasan Dağı (Tank and Karaş, 2020). Based on zircon age spectra modelling, it is hypothesized that melt pockets underneath Erciyes Dağı are small and disconnected, and thus difficult to geophysically resolve. For both volcanoes, future eruptions are anticipated, with Hasan Dağı being more predictable based on an eruptive recurrence interval of 5–15 ka over the past c. 100 ka, whereas high magma flux episodes at Erciyes Dağı are intermittent and occurred only twice in the same time interval. The quasi-synchronous dome eruptions in the periphery of Erciyes Dağı at c. 8.9 ka (Friedrichs et al., 2020) indicate that such a surge in magma recharge can result in major volcanic hazards.

Acknowledgments: this presentation is based on collaborative research and many discussions with Bjarne Friedrichs, Oscar Lovera, and Gökhan Atıcı.

REFERENCES

- Boehnke, P., Watson, E.B., Trail, D., Harrison, T.M. and Schmitt, A.K., 2013. Zircon saturation re-revisited. *Chemical Geology*, <https://doi.org/10.1016/j.chemgeo.2013.05.028>.
- Friedrichs, B., Atıcı, G., Danišík, M., Yurteri, E. and Schmitt, A.K., 2021. Sequence modeling in zircon double-dating of early Holocene Mt. Erciyes domes (Central Anatolia). *Quaternary Geochronology*, <https://doi.org/10.1016/j.quageo.2020.101129>.
- Friedrichs, B., Schmitt, A.K., Lovera, O.M. and Atıcı, G., 2021. Zircon as a recorder of contrasting magma recharge and eruptive recurrence patterns. *Earth and Planetary Science Letters*, <https://doi.org/10.1016/j.epsl.2021.117104>.
- Harrison, T.M., Watson, E.B. and Aikman, A.B., 2007. Temperature spectra of zircon crystallization in plutonic rocks. *Geology*, <https://doi.org/10.1130/G23505A.1>.
- Tank, S.B. and Karaş, M., 2020. Unraveling the electrical conductivity structure to decipher the hydrothermal system beneath the Mt. Hasan composite volcano and its vicinity, SW Cappadocia, Turkey. *Journal of Volcanology and Geothermal Research*, <https://doi.org/10.1016/j.jvolgeores.2020.107048>.
- Tierney, C.R., Schmitt, A.K., Lovera, O.M. and de Silva, S.L., 2016. Voluminous plutonism during volcanic quiescence revealed by thermochemical modeling of zircon. *Geology*, <https://doi.org/10.1130/G37968.1>.
- Weber, G., Caricchi, L., Arce, J.L. and Schmitt, A.K., 2020. Determining the current size and state of subvolcanic magma reservoirs. *Nature communications*, <https://doi.org/10.1038/s41467-020-19084-2>.

Zircon U-Pb dating method for the solution of geological problems in the menderes massif (western TÜRKIYE): example of the age of granulite-facies metamorphism

O.Ersin KORALAY^{1*}, Osman CANDAN¹, Qiu-Li LI², Fukun CHEN³, Yusheng WAN⁴, Alan S.COLLINS⁵

¹ Department of Geology, Engineering Faculty, Dokuz Eylül University, Tinaztepe Campus, Buca, 35160, Izmir, Türkiye

² State Key Laboratory of Lithospheric Evolution, Institute of Geology and Geophysics, Chinese Academy of Sciences, Beijing 100029, China,

³ Key Laboratory of Crust-Mantle Materials and Environments, School of Earth and Space Sciences, University of Science and Technology of China, Hefei, 230026, China

⁴ Beijing SHRIMP Center, Institute of Geology, Chinese Academy of Geological Sciences, 26 Baiwanzhuang Road, Beijing, 100037, China

⁵ Mawson Geoscience Centre and Department of Earth Sciences, University of Adelaide, Adelaide, SA 5005, Australia

ersin.koralay@deu.edu.tr

Abstract

The late Neoproterozoic poly-metamorphic basement of the Menderes Massif can be divided into two units (Bozdeğ Unit and Birgi Unit) with distinct metamorphic and magmatic histories. Birgi Unit consists of high-grade paragneiss - schist intercalation and (meta) acidic – basic intrusions. Granulite facies metamorphism has been preserved only in a few localities and is characterized by the orthopyroxene relics. Pelitic granulites and hypersthene orthogneisses (charnockites) form the main lithologies. The zircons in charnockites contain featureless overgrowth and rim textures representing metamorphic growth on magmatic cores and inherited grains. The protolith of the charnockites, yielded a crystallization age of ~ 590 Ma. U/Pb SHRIMP and LA-ICP-MS zircon and monazite ages from granulitic rocks gave an age of ca. ~580 Ma, which is interpreted as the time of granulite-facies metamorphism in the basement of the Menderes Massif. These data indicate that the Menderes Massif experienced acidic magmatic activity and granulite-facies metamorphism in Ediacaran. Furthermore, the basement rocks have been overprinted by a Barrovian-type Alpine metamorphism in Eocene (~ 42 Ma). The granulite-facies metamorphism in the Menderes Massif can be attributed to the orogenic event (600-500 Ma; Malagasy orogeny) causing the final amalgamation processes for the northern part of the Gondwana.

Keywords: Zircon U-Pb dating, Granulite-Facies Metamorphism, Menderes Massif, Gondwana

1. Introduction

The Menderes Massif (MM) in western Anatolia substantially shows a complex tectono-stratigraphy as a result of late Alpine compressional tectonics. This crystalline complex is tectonically overlain by the Afyon Zone in the northeast, east, and south, and the eastward continuation of the Cycladic Complex in Turkey in the west and northwest. It is covered by Neogene sedimentary/volcanic units (Figure 1a). The Menderes Massif is made up of an Ediacaran – early Cambrian basement and unconformably overlying Paleozoic – early Paleogene cover series (Figure 2). New field evidence and age data indicate that the Precambrian basement of the MM can be divided into two tectonic units; i) Bozdağ Unit (632 – 627 Ma) and ii) Birgi Unit (590-535 Ma). Both units are unconformably overlain by common upper Permian metamorphic cover indicating the tectonic juxtaposition before latest Paleozoic. Bozdağ Unit (older than 630 Ma) is made up of a continuous metasedimentary succession which is dominated by metapelites at the lower levels and passes upwards into marbles with a transition zone composed of black quartzites, phyllite and dolomite intercalation. Additionally, it contains acidic and basic magmatic rocks dated at 632-627 Ma and has subjected to a single-stage Alpine metamorphism (Eocene) under lower greenschist- to upper amphibolite-facies conditions. Tectonometamorphic evolution of the Bozdağ Unit is out of scope of this study. Birgi Unit composes of partially migmatized paragneisses and metapelites forming a regular and continuous sequence. Granitoid and gabbroic rocks have intruded into this metaclastic sequence at various stages of the Malagasy (Pan-African) orogeny. Relict mineral assemblages representing the granulite-, eclogite-, and amphibolite-facies conditions clearly reveal the polyphase metamorphic character of the Birgi Unit (Candan and Dora, 1998; Candan et al. 1995, 2001, 2011, 2016a; Oberhänsli et al., 1997; Koralay, 2015). The intrusion ages of granitoid and gabbroic rocks and the times of the polyphase metamorphisms affecting the basement rocks have been a matter of interest for a long time. Although the geochronological studies in the MM started before the 2000s and have increased until today, when considering the complex tectono-metamorphic history of the MM, more precise dating studies are still needed (Figure 2). It can be seen that U-Pb dating methods from minerals such as zircon and monazite offers the best solution to understanding this complex magmatic – metamorphic evolution. In the following sections, studies on the intrusion ages of the charnockitic granitoids and the ages of the granulite-facies metamorphism affecting the Birgi Unit of basement will be

summarized. This study is mainly based on the paper published by Koralay (2015) and additionally, previously unpublished data is compiled.

2. Methods

Heavy minerals were obtained using routine procedures that involved steel jaw-crusher, steel roller-mill, wilfley table and magnetic separator. Zircon concentrates separated from the non-magnetic fraction using heavy liquids, and single zircons were then handpicked under a binocular microscope at the Department of Geological Engineering, Dokuz Eylül University-Türkiye. Zircon grains studied by cathodoluminescence (CL) were mounted in epoxy resin discs and polished down to expose the grain centers. CL images were obtained on a microprobe CAMECA SX51 at the Institute of Geology and Geophysics, Chinese Academy of Sciences (IGG CAS) and on the Phillips XL40 SEM with attached Gatan CL at the University of Adelaide.

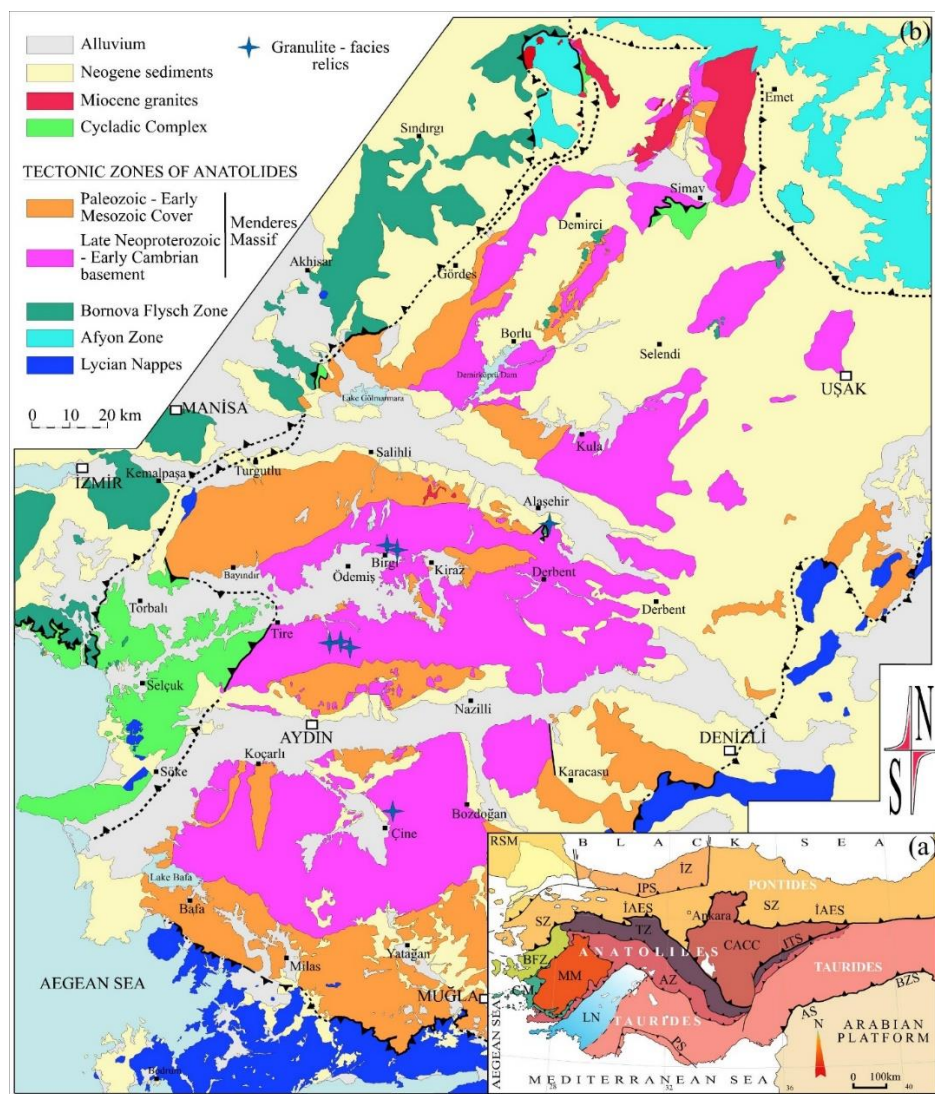


Figure 1. a) Tectonic map of Türkiye showing major continental blocks and tectonic zones (modified from Candan et al. 2016b). b) General distribution of basement and cover series of the Menderes Massif and localities of granulite-facies rocks.

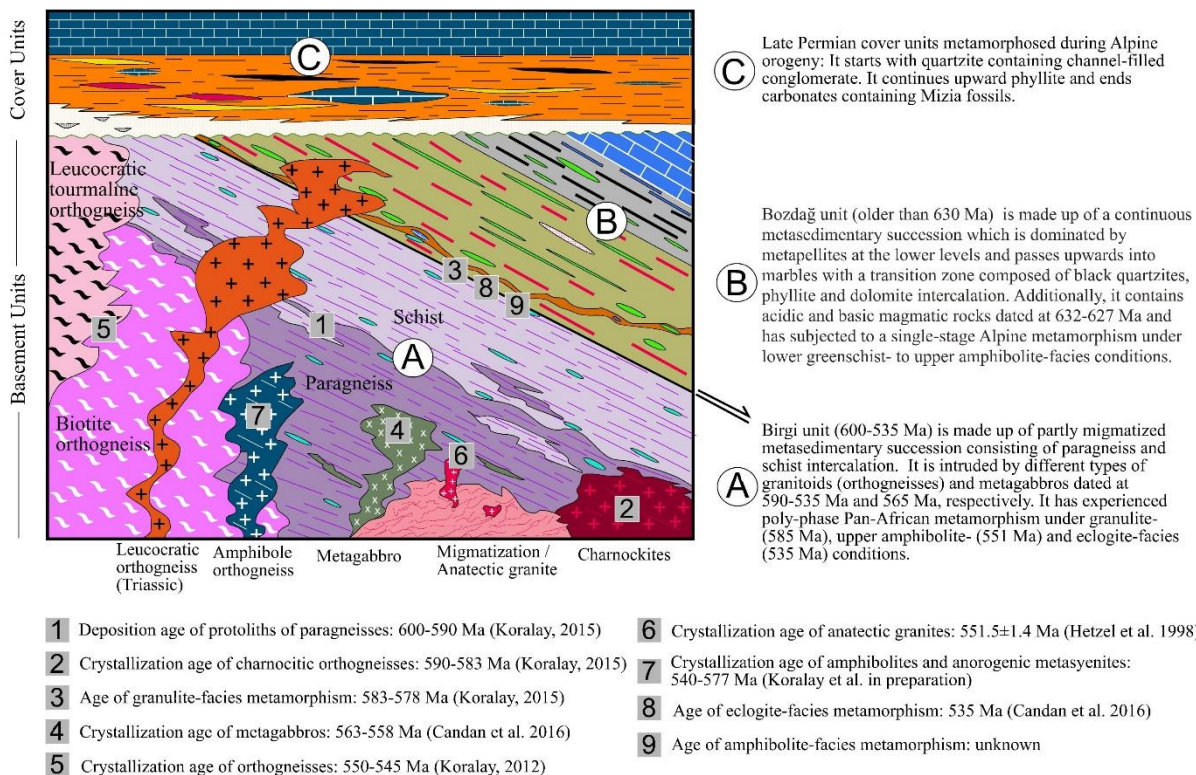


Figure 2. The generalized columnar section of the MM and magmatic and metamorphic events observed in the Birgi Unit of the massif (modified from Koralay et al. 2021).

Isotope Dilution Method: Zircons from metagranodiorite (type-1 charnockite / 05-2) were dated by the conventional U-Pb isotopic dilution method. For the conventional U-Pb isotopic dilution analyses, a standard cleaning procedure was applied in Chinese Academy of Sciences in Beijing-China. The detailed analytical procedures are given in Akal et al. (2012).

Pb-Pb Evaporation Method: Zircons from metagranodiorite (type-1 charnockite / 05-2) were dated by the Pb-Pb evaporation method. Isotope measurements of zircon were performed on a GV IsoProbe-T mass spectrometer by single-zircon evaporation in the Institute of Geology and Geophysics, Chinese Academy of Sciences in Beijing. The detailed analytical procedures are given in Akal et al. (2012).

SHRIMP Method: Zircons from metagranodiorites (type-1 charnockite / 05-2 and type-2 charnockite / 371) were dated by Sensitive High Resolution Ion Microprobe Mass Spectrometer (SHRIMP) at the Beijing SHRIMP Centre, Institute of Geology, Chinese Academy of Geological Sciences. The detailed analytical procedures are given in Koralay (2015).

LA-ICP-MS Method: Zircon dating of metagranodiorites (type-2 charnockite / 371, orthopyroxene metatonalite and type-3 charnockite / 12-28) were performed by Laser Ablation Inductively Coupled Plasma Mass Spectrometer (LA-ICPMS) at University of Science and

Technology of China in Hefei, using an ArF excimer laser system (GeoLas Pro, 193nm wavelength) and a quadruple ICP-MS (PerkinElmer Elan DRCII). The detailed analytical procedures are given in Koralay (2015).

3. Geology and mineralogy of granulite-facies rocks

The generalized lithostratigraphy of the Birgi Unit consists of a thick metaclastic sequence and voluminous syn- to post-metamorphic acidic and basic intrusions (Dora et al. 2001; Candan et al. 2011a, 2011b, 2016a; Koralay et al. 2012). The metaclastic sequence consisting of locally migmatized paragneisses and overlying mica schists forms the oldest unit. Based on the geochronological data, the depositional age of the protoliths of the paragneiss-schist sequence is constrained between 600 Ma and 590 Ma, i.e., Ediacaran (Koralay et al. 2012). These basement rocks showing high-grade metamorphisms are intruded by the protoliths of orthogneisses. Based on the mineralogical compositions and textural properties, different types of orthogneisses have been distinguished: biotite-, leucocratic tourmaline-, and amphibole-orthogneisses (Bozkurt, 2004; Candan et al. 2011b; Koralay et al. 2012). In addition, apart from these orthogneiss types, the existence of orthopyroxene-bearing orthogneisses which is the subject of this study has been documented (Candan 1995; Candan and Dora 1998; Koralay 2015). The U/Pb and Pb/Pb zircon ages of orthogneisses cluster at around ~ 550-537 Ma and are interpreted as intrusion ages of the granitic precursors of the orthogneiss (Hetzl and Reischmann 1996; Loos and Reischmann, 1999; Gessner et al. 2004; Candan et al. 2011a; Koralay et al. 2004, 2011, 2012). They are interpreted as syn- to post-magmatic intrusions, related to the latest Neoproterozoic final amalgamation of the Gondwana (Hetzl and Reischmann 1996; Candan et al. 2011b,c; Koralay et al. 2011, 2012). Additionally, the basement series are intruded by numerous poly-metamorphic basic intrusions occurring as stocks and veins. These well-preserved olivine- and biotite-gabbros were locally converted into eclogitic metagabbros and garnet amphibolites along the contacts or internal shear zones. U-Pb dating of igneous zircons from gabbroic rocks yielded ages of 563-558 Ma, indicating emplacement during the Ediacaran. On the other hand, rims of zircons from eclogitic metagabbro gave 535 ± 3 Ma ages interpreted as the time of eclogite-facies metamorphism (early Cambrian).

The relics of phases indicating a granulite-facies metamorphism are very rare in the MM and are best preserved in Tire and Birgi areas (Figure 1b). The granulite-facies metamorphism is

mainly recognized by rare orthopyroxene relics and pseudomorphic cordierite porphyroblasts (Candan, 1995; Candan and Dora, 1998; Dora et al. 2001; Koralay, 2015). Two main types of granulitic rocks have been distinguished. These are; i) pelitic granulites with orthopyroxene and ii) charnockites which were derived from granitoids (Figure 3). Based on the protolith, textural characteristic and mineralogical composition, three types of charnockites can be distinguished (type-1: massive, medium-grained metagranodiorite, type-2: granodiorite with gneissose texture, and type-3: coarse-grained metatonalite) (Candan and Dora, 1998; Koralay, 2015). The type-1 is sillimanite-rich, medium- to coarse-grained massive rock with orthopyroxene crystals, up to 3 mm in size (Figure 3a). They consists of quartz, plagioclase, orthoclase, orthopyroxene (hypersthene), garnet, sillimanite, and biotite. Whereas, type-2 rocks are characterized by a gneissose texture with bluish orthoclase porphyroclasts, up to 5 cm in diameter, (Figure 3c). They include partly assimilated paragneiss enclaves, up to 100 m, and show a primary intrusive contact relationship with paragneisses. Their mineral assemblage can be given as quartz, plagioclase, orthoclase, orthopyroxene, garnet, and biotite. Metatonalites (type-3) are coarse-grained, dark, and massive rocks with orthopyroxene crystals, up to 1cm (Figure 3d). The granulite-facies assemblage of metatonalite is quartz, plagioclase, orthopyroxene, biotite, rutile, and ilmenite. Moreover, these high-grade rocks are cut by numerous meta-gabbroic stocks and sill-like bodies of *ca.* 565 Ma (Candan et al. 2016a). They have not been affected by granulite facies metamorphism indicating that they postdate the high-T metamorphism.

Pelitic granulites are massive to weakly foliated rocks with fine-grained granoblastic texture (Figure 4). The granulite-facies mineral assemblage is quartz, plagioclase, orthoclase, orthopyroxene, garnet, biotite and rutile. Textural evidence clearly shows the widespread overprinting of granulitic assemblages under upper amphibolite facies conditions. During this overprint, orthopyroxenes are widely consumed by fine-grained biotite. Similarly, biotite porphyroblasts are recrystallized to fine-grained new biotite aggregates or are partially replaced by plagioclase-biotite symplectites. Granulitic garnet occurs as xenoblastic porphyroblasts with quartz inclusions and is essentially almandine-pyrope solid solutions with minor grossular and spessartine components. Furthermore, they are surrounded by fine grained new garnet crystals developed during the retrograde overprint. The same garnet coronas can also be seen around orthopyroxene and biotite. Sillimanite is closely associated with biotite and occurs as fibrolite and small prismatic crystals (Candan, 1995; Koralay, 2015). In the previous studies, based on geological relationships, an age between Cambrian–Ordovician has been assumed for granulite facies metamorphism (Candan, 1995). P-T conditions for this high-T event were estimated at

about 730–760 °C and 6 kbar (Candan and Dora, 1998; Candan et al. 2011). Both type-1 and type-2 charnockites have similar compositions and plot into granodiorite field, on the other hand, type-3 charnockites are mainly tonalitic in composition (Koralay, 2015).

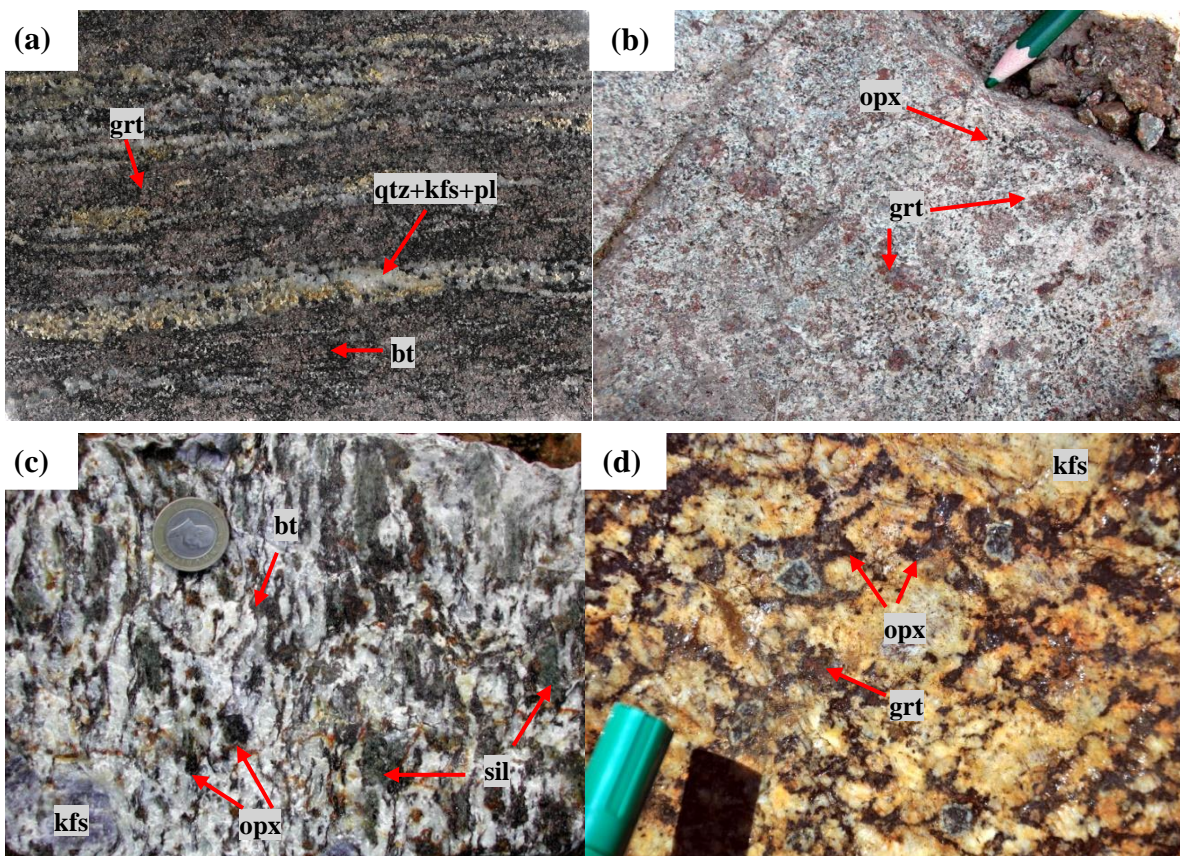


Figure 3. a) Fine-grained pelitic granulite, b) type-1: massive, medium-grained metagranodiorite, c) type-2: granodiorite with gneissose texture, and d) type-3: coarse-grained metatonalite (modified from Koralay, 2015). bt: biotite, grt: garnet, kfs: orthoclase, opx: orthopyroxene, pl: plagioclase, qtz: quartz, sil: sillimanite.

4. Geochronology

4.1. Previous Geochronological Studies on Granulite-Facies Rocks

In previous studies, the age of ca. 500 Ma (Cambrian-Ordovician) has been envisaged for granulite-facies metamorphism based on geological relationships (Candan, 1995). There are very limited geochronological age data obtained from the high-T rocks of the basement. Oelsner et al. (1997) has obtained a monazite age of $660 + 61/-63$ Ma by the electron microprobe Th-U-Pb method indicating that the age of the granulite-facies metamorphism is at least Precambrian, although the error obtained from monazites by Oelsner et al. (1997) is very high.

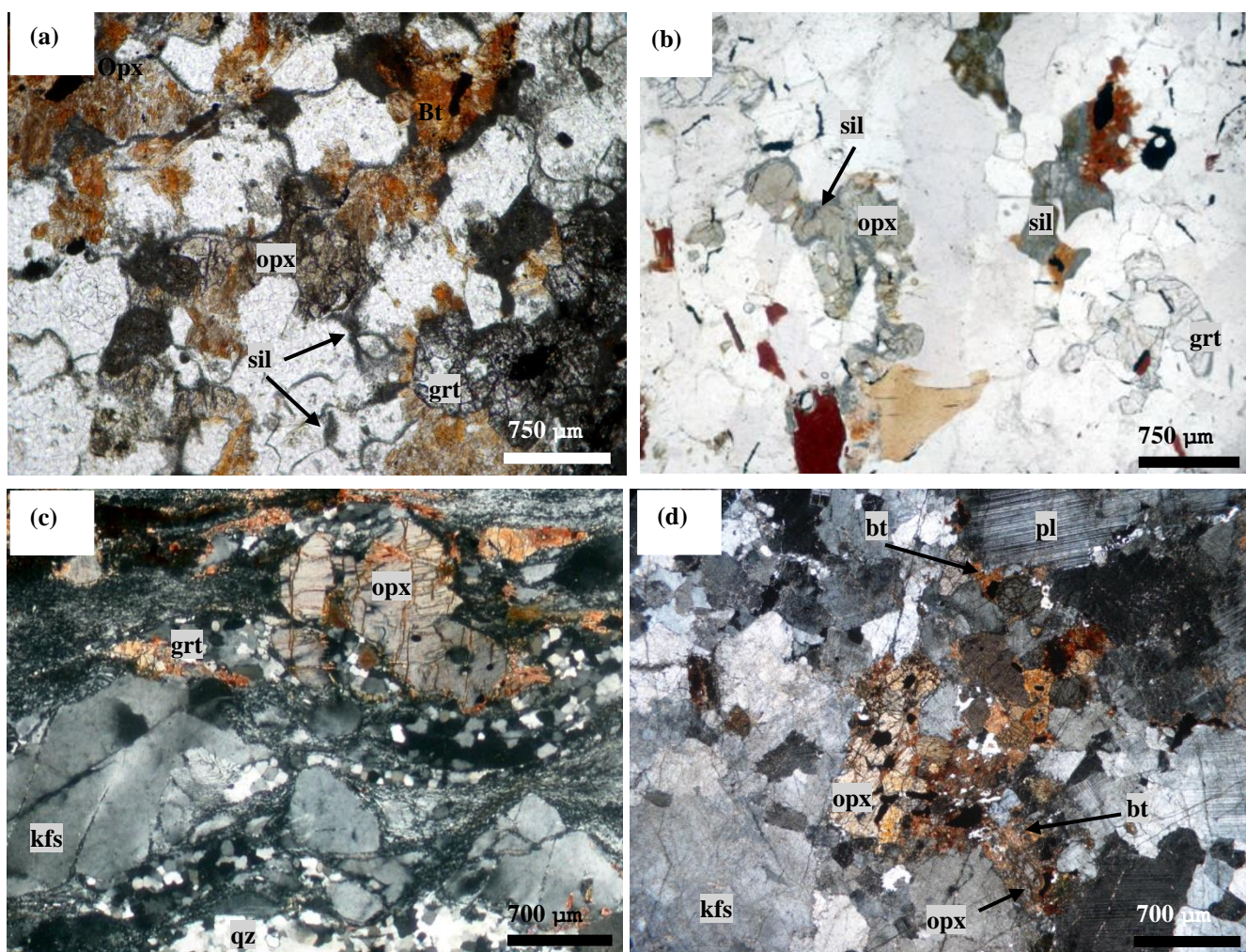


Figure 4. Generalized microscopic views of a) pelitic granulite, b) Type-1 charnockitic metagranodiorite, c) Type-2 charnockitic metagranodiorite, and d) Type-1 charnockitic metatonalite. Mineral abbreviations are the same as in Figure 3 (modified from Koralay, 2015).

4.2. Geochronological Methods Applied to Granulite-Facies Rocks

To better approximate the age of granulite-facies metamorphism in the MM, several different methods were applied. First, the U-Pb isotope dilution method was tried on different zircon populations. Four different zircon populations yielded a lower intercept age of 612 ± 12 Ma in the concordia diagram (Figure 5). This age has been interpreted as the age of granulite-facies metamorphism. Later, the single zircon evaporation method had been widely used for dating of high-T and ultra-high-T rocks such as granulites and charnockites for many years before more modern methods such as SHRIMP and LA-ICP-MS emerged (Kröner et al. 1997, 2015; Sommer and Kröner, 2015). The reason why this method has been preferred for many years is that the round, multi-faceted grains represent typical granulite-facies zircons (Figure 6, Wu and Zheng, 2004). Based on this general view, four round and multi-faceted zircon grains from the

study area were selected and their ages were determined by ^{207}Pb - ^{206}Pb single-zircon evaporation method. One of these grains (grain 1) yielded an age of 590 ± 7 Ma at five different temperature steps (Table 1). The age of 590 ± 7 Ma can be interpreted as the age of granulite-facies metamorphism of this sample.

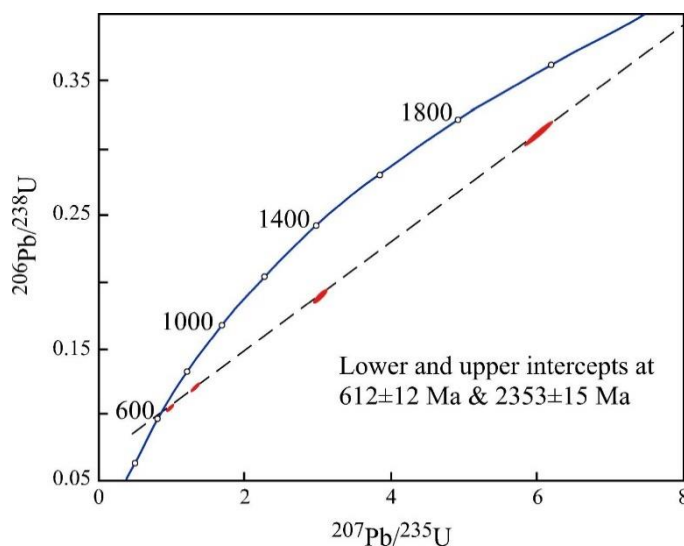


Figure 5. Concordia diagram showing isotope dilution analyses of four different zircon populations. Ellipses shown represent 95% confidence limits.

Table 1. Metamorphic zircon $^{207}\text{Pb}/^{206}\text{Pb}$ ratios obtained by the evaporation method and corresponding ages. mf: multi-faceted, e: ellipsoidal, y: yellowish, cl: clear, tr: transparent, l: large, m: medium.

Sample number	Zircon definition	Grain	Number of steps	$^{207}\text{Pb}/^{206}\text{Pb}$ ratios (weighted)	weighted $^{207}\text{Pb}/^{206}\text{Pb}$ plateau age
05-02	mf, e, y, cl, tr, l	1	5	0.059594 ± 0.000019	589.9 ± 6.9
	mf, e, y, cl, tr, l	2	3	0.063421 ± 0.000046	722.4 ± 15.0
	mf, e, y, cl, tr, m	3	5	0.064230 ± 0.000025	749.2 ± 8.2
	mf, e, y, cl, tr, m	4	2	0.219674 ± 0.000076	2978.3 ± 5.6

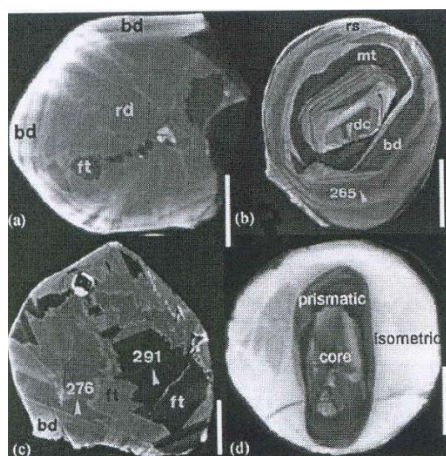


Figure 6. Typical granulite-facies metamorphic zircon CL images, a) Sector zoning, b) planar zoning, c) fir-tree zoning, d) no or weakly zoning. All images are taken from Vavra et al. (1996, 1999).

CL studies on these zircons in the following years revealed that they might have an extremely complex internal structure (Figure 7). The textural characteristics of these zircon grains can be given as; i) many of the grains contain irregular, bright luminescent featureless rims representing metamorphic growth around inherited cores, ii) Cores of the zircons have angular and fractured shapes with no zoning, flow zoning, oscillatory zoning, and sector zoning. Some of the cores have euhedral and multifaceted shapes reflecting typical metamorphic growth and display sector zoning and fir-tree zoning, iii) The majority of zircons show oscillatory and planar-zoned overgrowths representing crystallization from anatetic melts. Textural relationships clearly reveal that granulite-facies unzoned zircon overgrowth should have occurred prior to planar-zoned overgrowth.

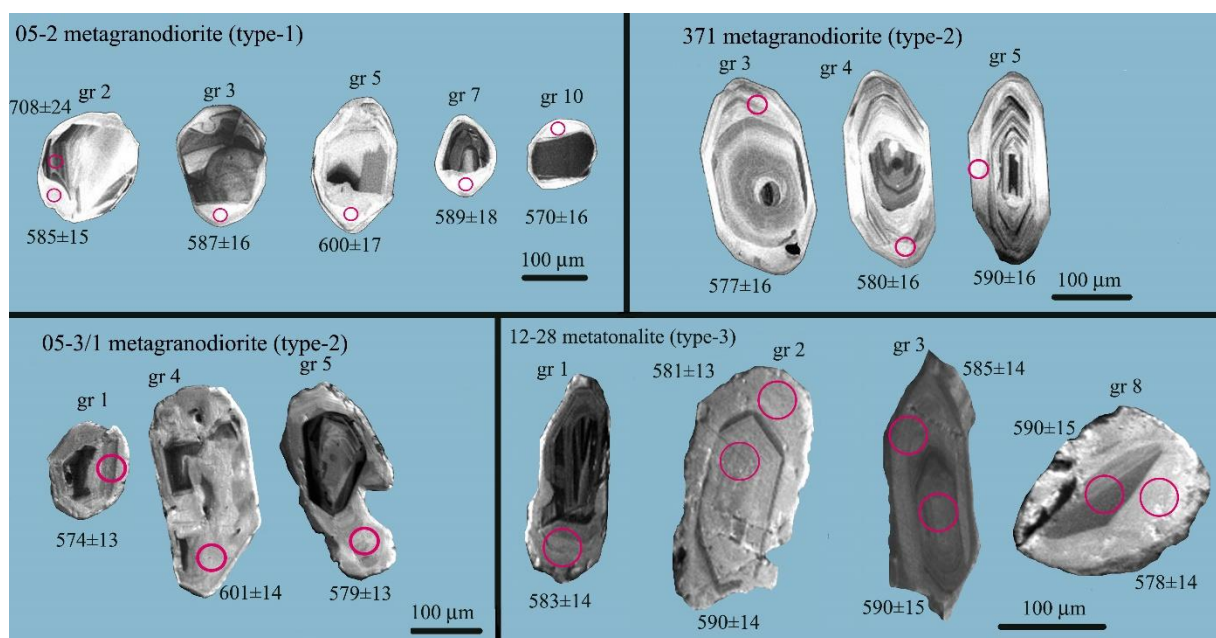


Figure 7. Cathodoluminescence (CL) images of the representative internal textures of typical zircon populations for metagranodiorite (type-1; 05-2), metagranodiorite (type-2; 371 and 05-3/1) and metatonalite (type-3; 12-28) (modified from Koralay, 2015).

Since a reliable age could not be obtained by the isotope dilution and Pb-Pb evaporation method, samples were dated using SHRIMP and LA-ICP-MS, which are the more advanced and reliable methods. Four samples, three charnockitic metagranodiorite (type-1 and type-2) and one charnockitic metatonalite (type-3), have been selected for age determinations. In order to find out the primary crystallization ages of the protoliths of the samples, core parts of the zircons showing typical oscillatory zoning were dated. Moreover, metamorphic overgrowths with Th/U ratios between 0.04 and 0.14, which are typical for metamorphic zircons (Wu and Zheng, 2004), were targeted. Magmatic domains yielded a $^{206}\text{Pb}/^{238}\text{U}$ weighted mean age of 591±6 Ma interpreted as the crystallization age of igneous precursor for type-3 charnockite (metatonalite) (Figure 8). The metamorphic rims yielded ages of 580±6 Ma, 582±9 Ma, 589±14 Ma, and 580±5 Ma from the samples 05-02, 371, 05-3/1, and 12-28, respectively (Figure 5; Koralay, 2015; see supplementary Table B). Moreover, one monazite grain yielded a weighted mean age of 578±3 Ma, which was dated by LA-ICP-MS from metagranodiorite (type-1, sample 05-2; Koralay, 2015; see supplementary Table D). This age is consistent with the U-Pb SHRIMP and LA-ICP-MS ages obtained from featureless rims of charnockitic samples. As a result, the age of ~ 580 Ma has been interpreted as the age of granulite-facies metamorphism affected the basement (Birgi Unit) of the Menderes Massif. Koralay (2015) reports biotite and whole-rock Rb-Sr isochron age of 42±1 Ma interpreted as the cooling age of the Alpine overprint on the basement.

5. Interpretation of age data and discussion

As known from previous studies, prior to the Eocene Alpine metamorphism, the basement of the Menderes Massif (Birgi Unit) has undergone a complex metamorphic history during the latest Neoproterozoic, which is ascribed to the assembly of Gondwana (Candan et al., 2011a and references therein). The metatonalite (type-3) sample from the Birgi region yields an age of 591 ± 6 Ma (Figure 8). Based on well-defined oscillatory zoning and high Th/U ratios of zircons, this age is interpreted as the protolith age of the metatonalite. However, the metamorphic zircons from other samples yielded ~ 580 Ma, which was interpreted as the age of granulite-facies metamorphism.

As it is emphasized in many studies, two tectonothermal events, ~ 650 - 620 Ma East African orogeny and ~ 600 - 500 Ma Malagasy-Kuunga orogeny, play a crucial role in the final configuration of the Neoproterozoic to Early Palaeozoic supercontinent Gondwana (Koralay, 2015 and references therein). Both orogenic events are characterized by the existence of widespread granulite-facies metamorphic rocks. In the Mozambique Belt of the East African Orogen, granulite-facies rocks have been documented in many places and their ages are between 652 Ma and 618 Ma. However, the Late Neoproterozoic to Cambrian granulite-facies metamorphism of the second major orogenic episode (Malagasy orogeny), which is located eastern part of the East African orogeny has been reported in many places and their ages range from 600 Ma to 520 Ma (Koralay, 2015 and references therein). The age of granulite-facies metamorphism (~ 580 Ma) in the Menderes Massif rules out a possible genetic relationship to the East African orogeny. However, there is a close relationship between the age of the granulite-facies metamorphism in the Menderes Massif and the high T metamorphism that developed as a result of the Malagasy orogeny (600-500 Ma). Considering the inferred latest Neoproterozoic - early Cambrian paleogeographic setting of the Anatolide-Tauride Block, the granulite-facies metamorphism in the Menderes Massif can be attributed to the northward continuity of Malagasy Orogen (Koralay, 2015 and references therein).

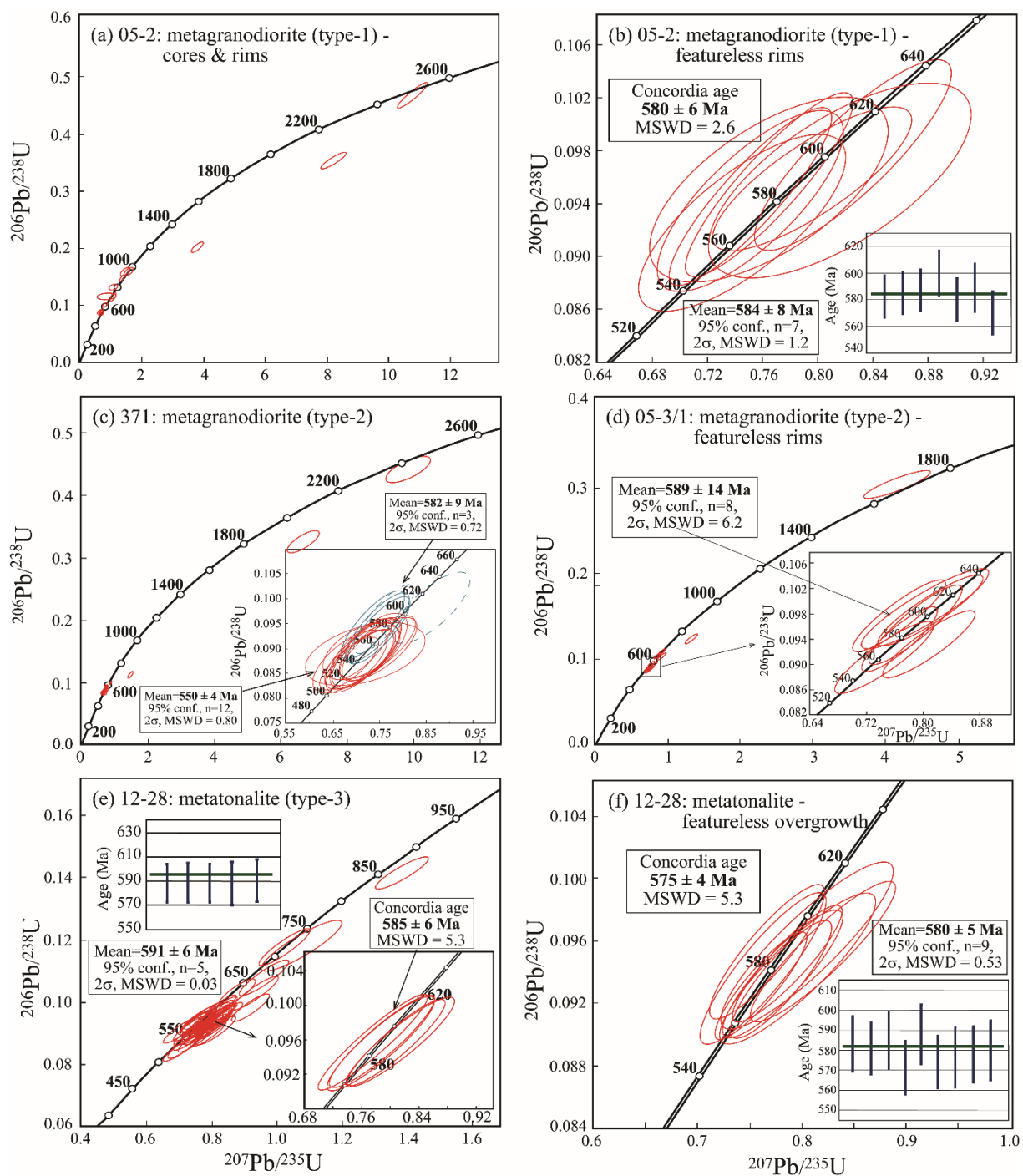


Figure 8. Zircon U-Pb concordia diagrams of metagranodiorite (type-1; 05-2), metagranodiorite sample (type-2; 371 and 05-3/1) and metatonalite sample (type-3; 12-28). All images are taken from Koralay (2015).

6. Conclusions

Mineralogical and textural evidence indicates the presence of former high-T metamorphism under granulite-facies conditions in the poly-metamorphic basement (Birgi Unit) of the Menderes Massif. Granulite-facies rocks in the Menderes Massif include orthopyroxene bearing pelitic granulites and charnockitic orthogneiss intrusions. U/Pb SHRIMP and LA-ICP-

MS zircon and monazite ages from granulitic rocks yield an age of ca. ~580 Ma, which can be interpreted as the time of granulite-facies metamorphism in the basement of the Menderes Massif. Moreover, the crystallization age of the protolith of the metatonalite, which experienced the granulite-facies metamorphism, has been determined as 591 ± 6 Ma. Granulitic rocks were overprinted by Alpine (Eocene; 42 Ma) metamorphism. Based on the inferred latest Neoproterozoic - early Cambrian paleogeographic position of the Anatolide-Tauride Block placed to the north of present-day Arabia, the granulite-facies metamorphism in the Menderes Massif can be attributed to the orogenic event (600-500 Ma; Malagasy orogeny) causing the final amalgamation processes for the northern part of the Gondwana.

Acknowledgements: This research was supported by Dokuz Eylül University research fund (BAP, project no: 04-KBFEN-088) and post-doctoral research fund of the Council of Higher Education (YÖK). We thank Zhenhui Hou for helping during the LA-ICP-MS measurements and Aoife McFadden and Adelaide Microscopy team for helping during CL imaging and the monazite measurement by LA-ICP-MS. Thanks are due to Gülin Gençoğlu Korkmaz for her editorial handlings.

REFERENCES

- Akal, C., Candan O., Koralay, O.E., Oberhänsli, R., Chen, F., Prelević, D., 2012. Early Triassic potassic volcanism in the Afyon Zone of the Anatolides/Turkey: implications for the rifting of the Neo-Tethys. *International Journal of Earth Sciences*, 101, 177-194.
- Bozkurt, E., 2004. Granitoid rocks of the southern menderes Masif (southwestern Turkey): field evidence for Tertiary magmatism in an extensional shear zone. *Int. J. of Earth Sciences*, 93, 52-71.
- Candan, O., 1995. Menderes Masifi'ndeki kalıntı granulit fasiyesi metamorfizması. *Turkish Journal of Earth Sciences*, 4, 35-55.
- Candan, O. and Dora, O.Ö., 1998. Menderes Masifi'nde granulit, eklojıt ve mavi sist kalıntıları: Pan- Afrikan ve Tersiyer metamorfik evrimine bir yaklaşım. *Türkiye Jeoloji Bülteni*, 41/1, 1-35.
- Candan, O., Dora, O.Ö., Oberhansli, R. and Dürr, St., 1995. Relicts of high-pressure metamorphism in the Menderes Massif: Eclogites. *International Earth Sciences Colloquium on the Aegean Region-1995*, Izmir-Turkey, Abstracts, 8-9.
- Candan, O., Dora, O.Ö., Oberhansli, R., Çetinkaplan, M., Partzsch, J.H., Warkus, F. and Dürr, St. 2001. Pan-African high-pressure metamorphism in the Precambrian basement

- of the Menderes Massif, Western Anatolia. Turkey. *Int. J. Earth Sci. (Geologische Rundschau)*, 89, 4, 793-811.
- Candan, O., Oberhänsli, R., Dora, O.Ö., Çetinkaplan, M., Koralay, E., Rimmele, G., Chen, F. and Akal, C., 2011a. Polymetamorphic evolution of the Pan-African basement and Palaeozoic-Early tertiary cover series of the Menderes Massif. *Mineral Res. Expl. Bull.*, 142, 121-163.
- Candan, O., Dora, O.Ö., Oberhänsli, R., Koralay, E., Çetinkaplan, M., Akal, C., Satır, M., Chen, F., and Kaya, O., 2011b. Stratigraphy of the Pan-African basement of the Menderes Massif and the relationship with late Neoproterozoic/Cambrian evolution of the Gondwana. *Mineral Res. Expl. Bull.*, 142, 25-68.
- Candan, O., Koralay, O.E., Topuz, G., Oberhänsli, R., Fritz, H., Collins, A.S., Chen, F., 2016a. Late Neoproterozoic gabbro emplacement followed by early Cambrian eclogite-facies metamorphism in the Menderes Massif (W. Turkey): Implications on the final assembly of Gondwana. *Gondwana Research*, 34, 158-173.
- Candan, O., Akal, C., Koralay, O.E., Okay, A.I., Oberhänsli, R., Prelević, D., Mertz-Kraus, R., 2016b. Carboniferous granites on the northern margin of Gondwana, Anatolide-Tauride Block, Turkey – Evidence for southward subduction of Paleotethys. *Tectonophysics*, 683, 349-366.
- Dora, O.Ö., Candan, O., Kaya, O., Koralay, E., Dürr, S., 2001. Revision of the so-called “leptite-gneisses” in the Menderes Massif: A supracrustal metasedimentary origin. *International Journal of Earth Sciences*, 89(4), 836-851.
- Gessner, K., Collins, A., Ring, U., Güngör, T., 2004. Structural and thermal history of a poly-orogenic basement: U/Pb geochronology of granitoids rocks in southern Menderes Massif, Western Turkey. *Jour. of Geol. Soc. London*, 161, 93-101.
- Hetzel, R., and Reischmann, T., 1996. Intrusion age of Pan-African augen gneisses in the southern Menderes Massif and the age of cooling after Alpine ductile extensional deformation. *Geological Magazine*, 133(5): 565 - 572
- Koralay, O.E., 2015. Late Neoproterozoic granulite facies metamorphism in the Menderes Massif, Western Anatolia/Turkey): implication for the assembly of Gondwana. *Geodinamica Acta*, 27 (4), 244-266.
- Koralay, O.E., Candan, O., Erkül, F., Uzel, B., 2021. Menderes ve Alanya Masiflerindeki Bazik Metamagmatik ve Şistlerin Jeokimyası ve Jeokronolojisi: Gondvana'nın Kuzey Kenarının Neoproterozoyik Evrimindeki Yerleri. TÜBİTAK, Proje no: 117Y346.
- Koralay, E., Dora, O.Ö., Chen, F., Satır, M., and Candan O., 2004. Geochemistry and geochronology of orthogneisses in the Derbent (Alaşehir) area, Eastern part of the Odemiş-Kiraz submassif, Menderes Massif: Pan-African magmatic activity. *Turkish Journal of Earth Sciences*, 13, 37-61.

- Koralay, O.E., Candan, O., Akal, C., Dora, O.Ö., Chen, F., Satır, M., and Oberhängsli, R., 2011. The geology and geochronology of the Pan-African and Triassic metagranitoids in the Menderes Massif, western Anatolia, Turkey. *Mineral Res. Expl. Bull.*, 142, 69-119.
- Koralay, E., Dora, O.Ö., Chen, F., Akal, C., Oberhängsli, R., Satır, M., Dora, O.Ö., 2012. Pan-African magmatism in the Menderes Massif,: geochronological data from leucocratic tourmaline orthogneiss in western Turkey. *International Journal of Earth Sciences*, 101, 2055-2088.
- Kröner, A., Sacchi, R., Jaekel, P., Costa, M. 1997. Kibaran magmatism and Pan-African granulite metamorphism in northern Mozambique: single zircon ages and regional implications. *Journal African Earth Sciences*, 25 (3), 467-484.
- Kröner, A., Santosh, M., Hegner, E., Shaji, E., Geng, H., Wong, J., Xie, H., Wan, Y., Shang, C.K., Liu, D., Sun, W., Nada-Kumar, V., 2015. Paleoproterozoic ancestry of Pan-African high-grade granitoids in southernmost India: Implications for Gondwana reconstructions. *Gondwana Research*, 27, 1-37.
- Loos, S., and Reischmann, T., 1999. The evolution of the southern Menderes massif in SW Turkey as revealed by zircon dating. *Jour. of Geol. Soc. London*, 156, 1021-1030.
- Oberhängsli, R., Candan, O., Dora, O.Ö., Dürr, St.H., 1997. Eclogites within the Menderes Massif/western Turkey. *Lithos*, 41 (1-3), 135-150.
- Oelsner, F., Candan, O ve Oberhängsli, R., 1997. New evidence for the time of the high grade metamorphism in the Menderes massif, Western-Turkey. *Geologische Verlinigung*, 1997, Zürich.
- Sommer, H., and Kröner, A., 2013. Ultra-high temperature granulite-facies metamorphic rocks from the Mozambique belt of SW Tanzania. *Lithos*, 170-171, 117-143.
- Vavra, G., Gebauer, D., Schmid, R., 1996. Multiple zircon growth and recrystallization during polyphase Late Carboniferous to Triassic metamorphism in granulites of the Ivrea Zone (Southern Alps): an ion microprobe (SHRIMP) study. *Contributions to Mineralogy and Petrology*, 122: 337_358
- Vavra, G., Schmid, R., Gebauer, D., 1999. Internal morphology, habit and U-Th-Pb microanalysis of amphibole to granulite facies zircon: geochronology of the Ivrea Zone (Southern Alps). *Contributions to Mineralogy and Petrology*, 134: 380-404.
- Wu, Y., Zheng Y., 2004. Genesis of zircon and its constraints on interpretation of U-Pb age. *Chenese Science Bulletin*, 49 (15), 1554-1569.

Düşük Sıcaklık Termokronolojisi ve Jeolojide Kullanımı

Fatih Karaoglan

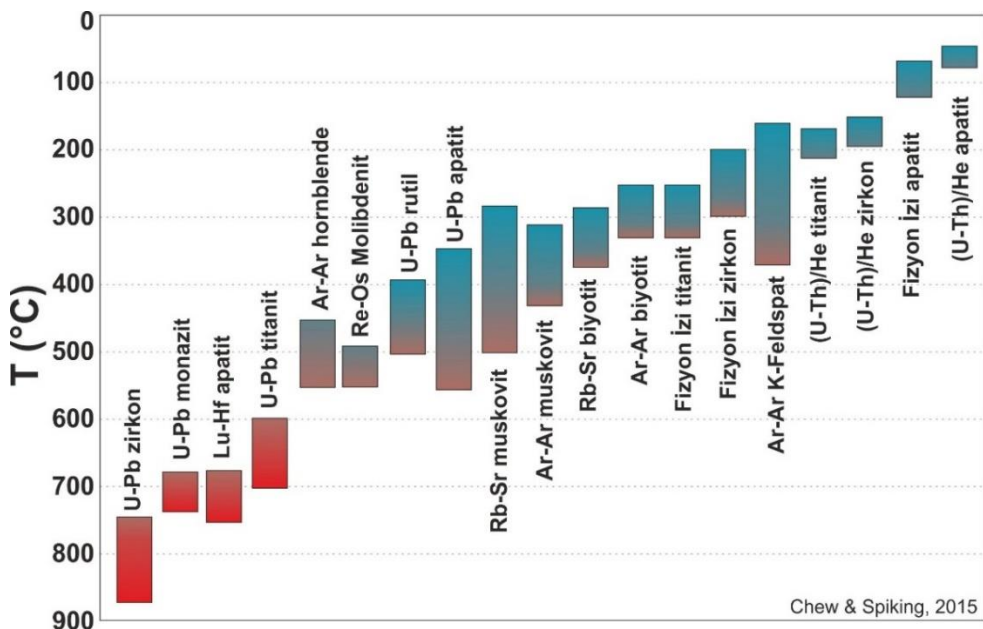
Çukurova Üniversitesi Mühendislik Fakültesi Jeoloji Mühndisliği Bölümü Balcalı 01330 Sarıçam Adana

Czech Academy of Sciences, Institute of Geology, Rozvojová 269, 165 00 Praha 6 - Lysolaje, Czech Republic

Jeokronoloji genel anlamda kayaçların oluşum yaşıının hesaplanması amaçlarken Termokronoloji kayaçların oluştuktuktan sonra termokronometrenin kapanma sıcaklığında ki soğumu yaşıının hesaplanması amaçlamaktadır. Düşük Sıcaklık Termokronolojisi ise kapanma sıcaklığı ~300-350°C'nin altında olan termokronometreler ile yapılan çalışmaları ifade etmektedir. Burada termokronometre olarak kullanılan materyal (tüm kaya ve/veya mineral) belirli bir sıcaklığın altında ölçülen radyoaktif (bozunan ana izotop) ve radyojenik (bozunma sonrası oluşan yavru izotop) izotoplardan için kapalı sistem özelliği taşımalıdır.

Düşük sıcaklık termokronolojisi kayaçların soğumaya başladığı zamanı ve genellikle soğuma hızının ölçülmesinde kullanılmaktadır. Kayaçlar genel olarak yüzeye yaklaştıklarında soğumaya başlarlar. Yüzeyleme süreci, erozyon veya faylanma ile gerçekleşebilir. Buna karşın Düşük Sıcaklık Termokronometreleri sıcaklığa duyarlı oldukları için kapanma sıcaklıklarına bindirme, naplaşma gibi tektonik olaylar, havzalarda sediman yükü altında gömülme veya magmatik sokulum ve ilişkili hidrotermal sıvıların etkisi ile ulaşılabilir ve termokronometreler bu olaylar ile sıfırlanabilir. Bir kayacın soğuması, yüzeyleme, akışkanlar, hidrotermal aktivetinin sonlanması ile jeotermal gradyanda düşme veya temel ısı akısında düşme ile gelişebilir (Ehlers, 2005; Peyton ve Carrapa, 2013). Yükselme (exhumation) kayacın yüzeye göre erozyonal süreçler veya tektonizma ile yukarıya doğru hareketi olarak tanımlanır (England ve Molnar, 1990). Aşınma/Erozyon (Denudation) ise yüzeyin kayaca göre aşağı doğru hareketi olarak tanımlanabilir (Peyton ve Carrapa, 2013).

Düşük Sıcaklık Termokronolojisi çalışmaları genel olarak Ar-Ar Biyotit termokronolojisi ve daha altında kapanma sıcaklığına sahip termokronoloji yöntemlerini içermektedir. Bunlar biyotit ve K-feldspar Ar-Ar ile apatit ve zirkon minerallerinde uygulanan Fizyon İzi (FT) ve (U-Th[-Sm])/He (He) yöntemlerini içermektedir (Şekil 1).Bunlar arasında en çok kullanılan yöntemler ise Fizyon izi ve ve (U-Th)/He yöntemleridir.



Şekil 1. Farklı jeokronoloji ve termokronoloji sistemlerinin kapanma sıcaklıkları (Chew ve Spikings, 2015).

Fizyon izi yöntemi apatit minerali için 100-120°C kapanma sıcaklığı ve 3-5.5 km kapanma derinliği, zirkon minerali için 210-300°C kapanma sıcaklığı ve 9.7-14.5 km kapanma derinliğine sahipken (U-Th)/He yöntemi apatit minerali için 55-75°C kapanma sıcaklığı ve 1.5-3.3 km kapanma derinliği, zirkon minerali için 1600-200°C kapanma sıcaklığı ve 5-9.5 km kapanma derinliğine sahiptir (Tablo 1)

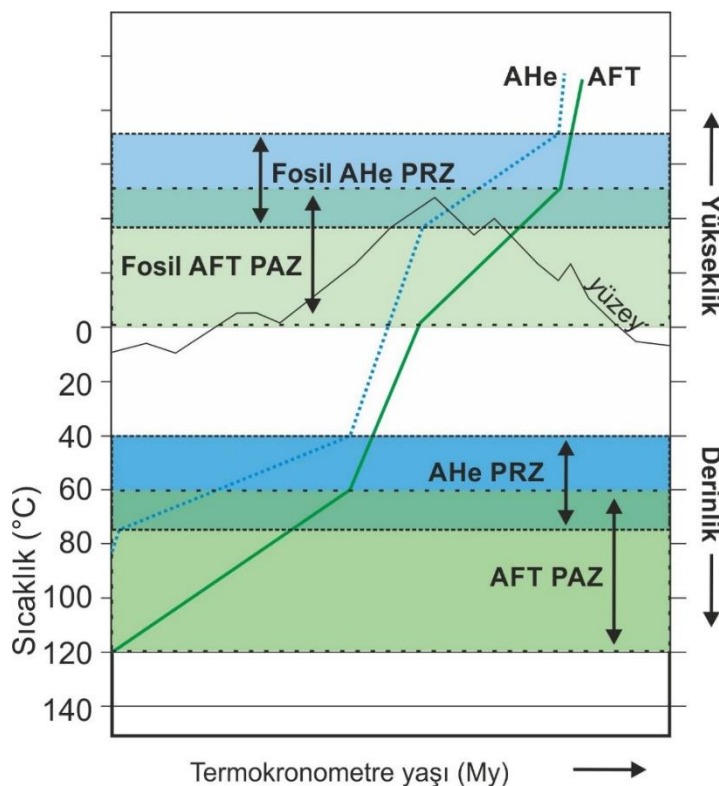
Tablo 1. Fizyon izi ve (U-Th)/He yöntemlerinin kapanma sıcaklıkları ve derinlikleri. Kapanma derinliği 20-30 °C/km jeotermal gradyon ve 10 °C yüzey sıcaklığı varsayılarak hesaplanmıştır (Enkelmann ve Garver, 2016).

Yöntem	Kapanma sıcaklığı (°C)	Kapanma derinliği (km)
Apatit (U-Th)/He	55-75	1.5-3.3
Zirkon (U-Th)/He	160-200	5-9.5
Apatit Fizyon İzi	100-120	3-5.5
Zirkon Fizyon İzi	210-300	9.7-14.5

Fizyon İzi yöntemi

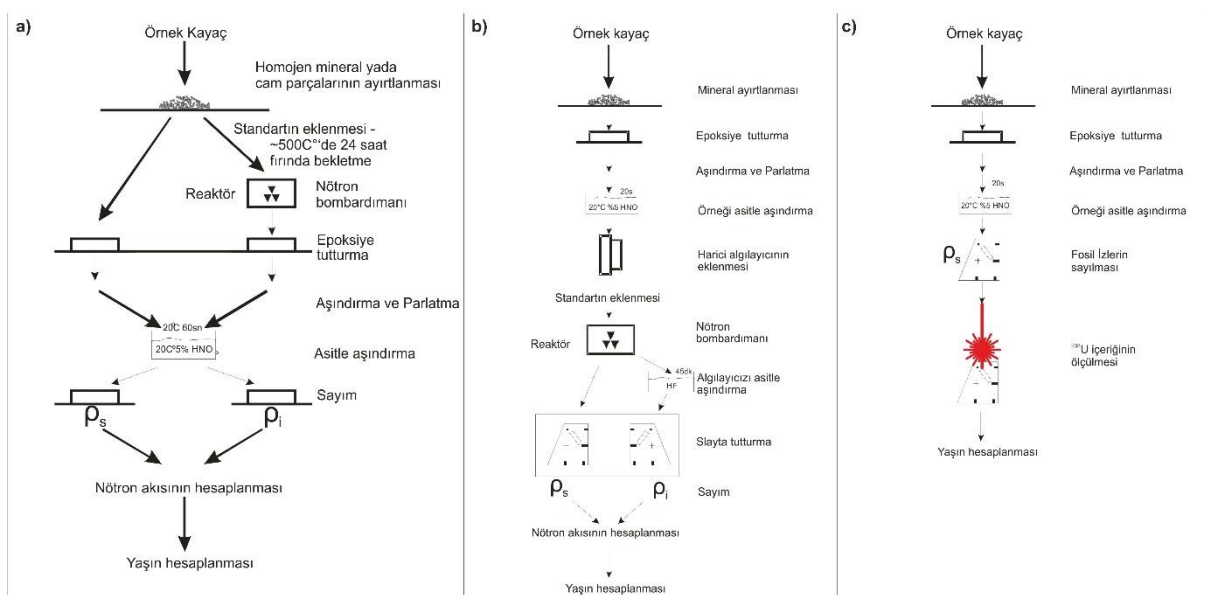
Düşük Sıcaklık Termokronolojisi yöntemleri genel olarak jeolojik zaman içinde yavru izotopu görece düşük sıcaklıklara (<300°C) duyarlı radyometrik tarihleme yöntemlerini içermektedir. Bunlardan apatit ve zirkon minerallerine uygulanan Fizyon İzi ve (U-Th-Sm)/He yöntemleri en yaygın olarak kullanılan yöntemlerdir. Her iki yöntemde bu minerallerde bulunan uranyumun radyoaktif bozunmasına dayanıp uranyum, toryum ve samaryumun α -bozunması

mineraller için He birikmesine sebep olurken uranyumun fizyon bozunması minerallerin kristal kafesinde hasara neden olur (Fleischer vd. , 1975; Zeitler vd. , 1987; Farley, 2002). Fizyon İzi yönteminde, apatit kristallerinde oluşan fizyon hasarı $\sim 120^{\circ}\text{C}$ üstünde bütün hasar (fizyon izleri) iyileşip kaybolur ve bunun sonu olarak da kristalin FT yaşı sıfır olur (Laslett vd. , 1987; Ketcham vd. , 1999). Bu durum zirkon kristalinde $\sim 240^{\circ}\text{C}$ üstünde gerçekleşir (Zaun ve Wagner, 1985; Reiners ve Ehlers, 2005; Peyton ve Carrapa, 2013). Kısmi iyileşme alanı (Partial Anealing Zone – PAZ) apatit mineralleri için kimyasal bileşimine bağlı olarak ~ 60 ile 120°C arasında iken zirkon minerallerinde 180 - 350°C arasındadır (Green vd. , 1989; Reiners ve Ehlers, 2005; Tagami, 2005) (Şekil 1,2, Tablo 1).



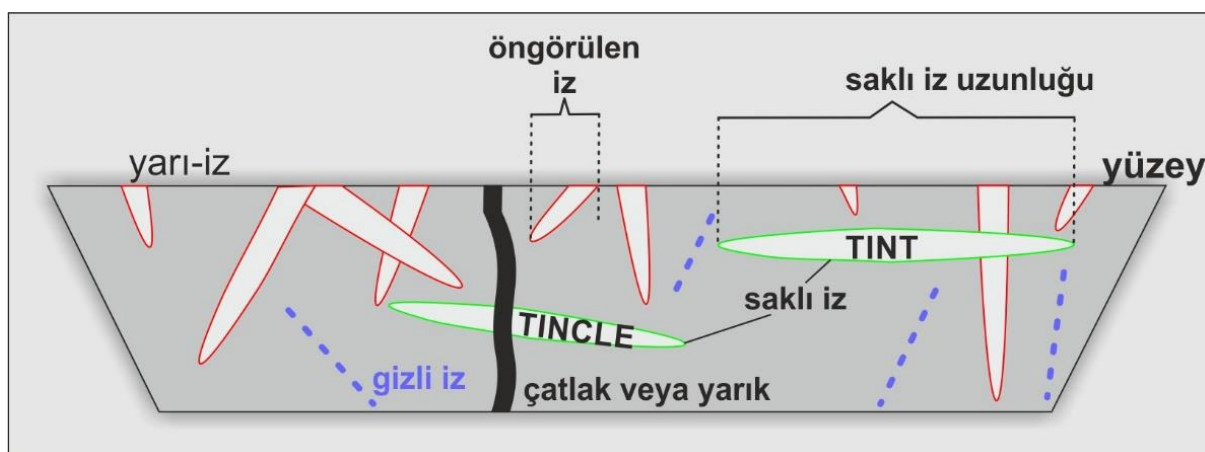
Şekil 2. Apatit Fizyon İzi Kısmi İyileşme Alanı (PAZ) ve apatit U-Th-Sm/He Kısmi Tutma Alanı (PRZ) (Armstrong, 2005; Peyton ve Carrapa, 2013).

Fizyon izi yaş tayini yönteminde çoklu tane veya tek tane üzerinden yaş tayini yapılmaktadır. Çoklu tane yönteminde bütün tanelerden sayılan izlerin ortalaması alınarak tek bir yaş elde edilirken, tek tane yönteminde her bir mineralden ayrı bir yaş hesaplanabilmektedir. Tek tane yöntemleri içerisinde günümüzde en yaygın kullanılan Harici Algılayıcı Yöntemi (External Detector Method – EDM) ve Lazer Ablasyon Fizyon İzi (LAFT) yöntemleridir (Şekil 3).



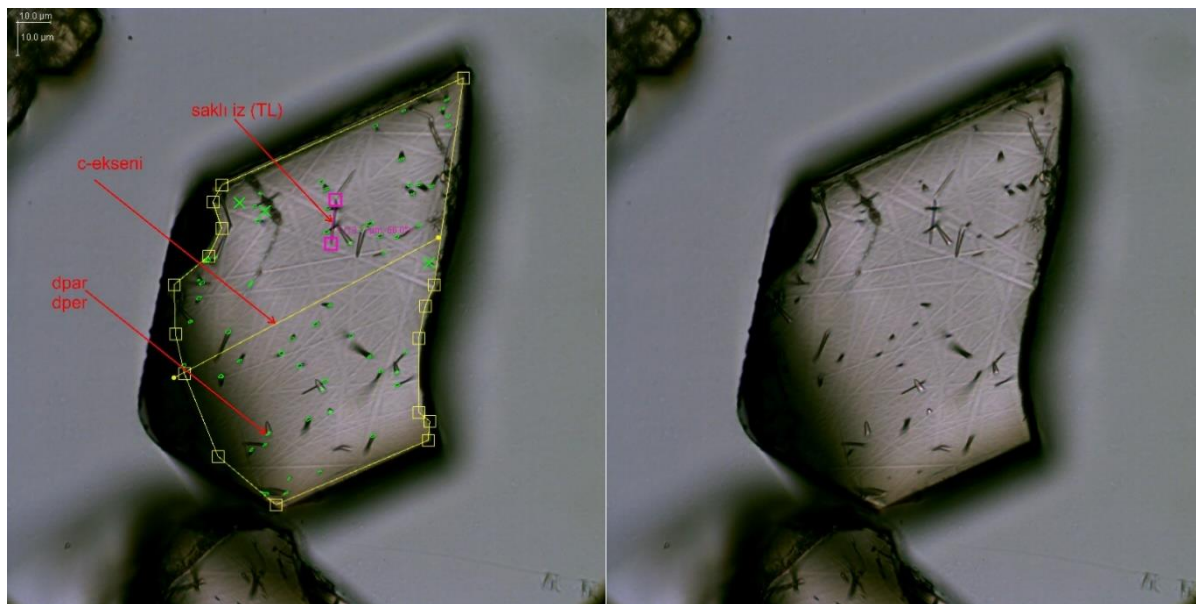
Şekil 3. Fizyon İzi tarihleme yöntemleri a) Çoklu tane yöntemi (Populated Granin Method-PGM), b) Harici Algılayıcı Yöntemi (External Detector Method-EDM), c) Lazer Aşındırma Fizyon İzi Yöntemi (Lazer Ablation Fission Track-LAFT).

Doğal veya reaktörde oluşan izler ancak elektron mikroskopu yardımı ile gözlenebilmektedir. Ancak basit bir kimyasal dağlama (etching) yöntemi ile izler optik mikroskop altında gözlenebilecek büyülükle erişebilir. Bunun için ayıklanan apatit (veya diğer mineraller) yüzeyleri epoksi reçine üzerine alındıktan sonra aşındırılıp parlatılır. Daha sonra kimyasal dağlayıcı yüzeye uygulandığında fizyon izlerinin parlatılmış yüzeyi kesitiği bölge genişleyerek elipsoid şeklinde 1-2 μm büyülükle erişir. Yüzeyin altında kalan izler optik mikroskop ile gözlenemez (Şekil 4).



Şekil 4. Apatit kristallerinde fizyon izleri, TINCLE (Track in Cleavage): çatlak ile kesişen iz, TINT (Track in Track): iz ile kesişen iz.

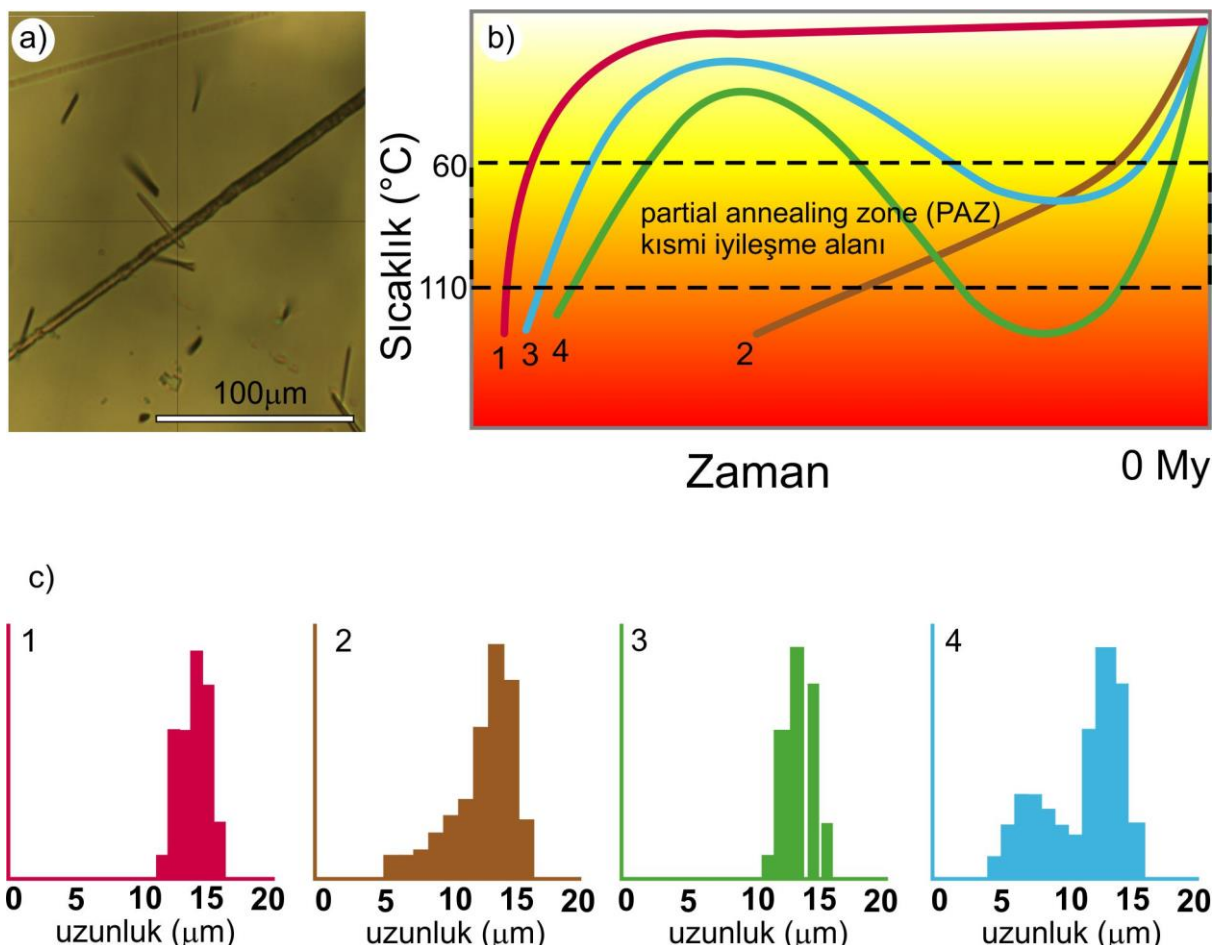
Apatit fizyon izi yönteminde elde edilen verilerin en önemlilerinden birisi ise örneğin 60-120°C arasında nasıl hareket ettiğini gösteren soğuma profilleridir. Bunun için örneğin yaşı, kinetik parametre (Cl içeriği veya DPar), saklı iz uzunluğu ve saklı izin c-ekseni ile yaptığı dar açı parametreleri kullanan yazılımlar kullanılmaktadır. Saklı izlerin dağılımına bakılarak da bu konuda fikir yürütülebilir (Şekil 4,5).



Şekil 5. Apatit kristallerinde gözlenen fizyon izleri ve ölçülen özellikler.

Saklı izler ilk oluşum anında 16-17 μm uzunluğunda olup ~120°C üzerinde bu izler iyileşerek kaybolurken ~60-120°C arasında izlerin boyaları kısalma eğilimdedirler. ~60°C altında ise izlerin boyalarının değişmediği varsayılmaktadır (Gleadow vd. , 1986a; Gleadow vd. , 1986b; Green vd. , 1986). Apatit kristallerinde saklı izler ölçüülerek örneğin ~60-120°C arası davranışını konusunda bilgi edilinebilir (Şekil 6). Aşağıda verilen şekilde (a) şeklinde kristal yüzeyinde bulunan çizik ile ilişkili saklı iz görünmektedir. Şekil 6b ve 6c ise farklı soğumu tarihçelerine sahip örneklerin oluşturabilecekleri soğuma prodilleri ile bunlara ait iz uzunluk dağılım histogramları görülmektedir. 1 nolu soğuma profili örneğin oluşumundan sonra hızlı soğuma ile PAZ alanını geçtiğini göstermektedir. Burada izlerin çoğunluğu PAZ alanını geçikten sonra oluşmuştur ve uzun saklı iz boyaları gözlenir. 2 nolu soğuma profili örneğin oluşumu sonucu yavaş soğumayı göstermektedir. Burada izler PAZ ve sonrasında oluşmuştur. Saklı izlerin PAZ alanında oluşanlar kısa sonrasında oluşanlar ise uzundur. 3 ve 4 nolu soğuma profillerinde örnek oluşumundan sonra PAZ alanının geçip tekrar ısınarak PAZ alanına girmiştir. 3 nolu soğuma profilinde karışık bir yaş verisi elde edilir. Önce oluşmuş izler PAZ alanında geçirdiği

süreye bağlı olarak kısalma gösterir. PAZ alanında son çıkıştan sonra uzun izler oluşur. 4 nolu soğuma profilinde ise örnek oluştuktan sonra PAZ alanı geçtikten sonra ısimmeye bağlı olarak PAZ alanının altına inmiş ve yaş verisi sıfırlanmıştır. Fizyon İzi yaşı son PAZ alanın alt sınırını geçtiği zamandır (Wagner ve Reimer, 1972; Gleadow vd. , 1986a; Gleadow vd. , 1986b).



Şekil 6. Saklı izlerin farklı soğuma koşullarına göre dağılımı (Wagner ve Reimer, 1972; Gleadow vd. , 1986b; Donelick vd. , 2005; Hurford, 2019).

(U-Th)/He Yöntemi

Yöntem asıl olarak U ve Th izotoplarının bozunması sırasında ${}^4\text{He}$ (alfa parçacığı) salması esasına dayanmaktadır (Tablo 2). U ve Th yanında Sm izotoplarında azda olsa alfa parçacığı salınımı vardır bu nedenle hene kadar yöntemin adı U-Th/He yöntemi olarak anılsa ve bu iki elementin izotoplarını ölçülmesi yeterli olsa da Sm izotoplarının ölçülebildiği yerlerde U-Th-Sm/He yöntemi olarak adlandırılabilir (Tablo 2).

Tablo 2. U-Th/He yönteminde alfa parçacığı salan izotoplar ve bozunmalar.

Ana izotop	Yavru izotop	Nb. α partikülleri	Yarılanma ömrü (Ga)
^{238}U	^{206}Pb	+ 8 α	(4.4683)
^{235}U	^{207}Pb	+ 7 α	(0.7038)
^{232}Th	^{208}Pb	+ 6 α	(14.05)
^{147}Sm	^{143}Nd	+ 1 α	(106)

Sistemdeki toplam ^4He miktarı aşağıdaki formül ile hesaplanır;

$$^4\text{He} = 8^{238}\text{U}(e^{\lambda_{238}t}-1) + 7^{235}\text{U}(e^{\lambda_{235}t}-1) + 6^{232}\text{Th}(e^{\lambda_{232}t}-1) + ^{147}\text{Sm}(e^{\lambda_{147}t}-1)$$

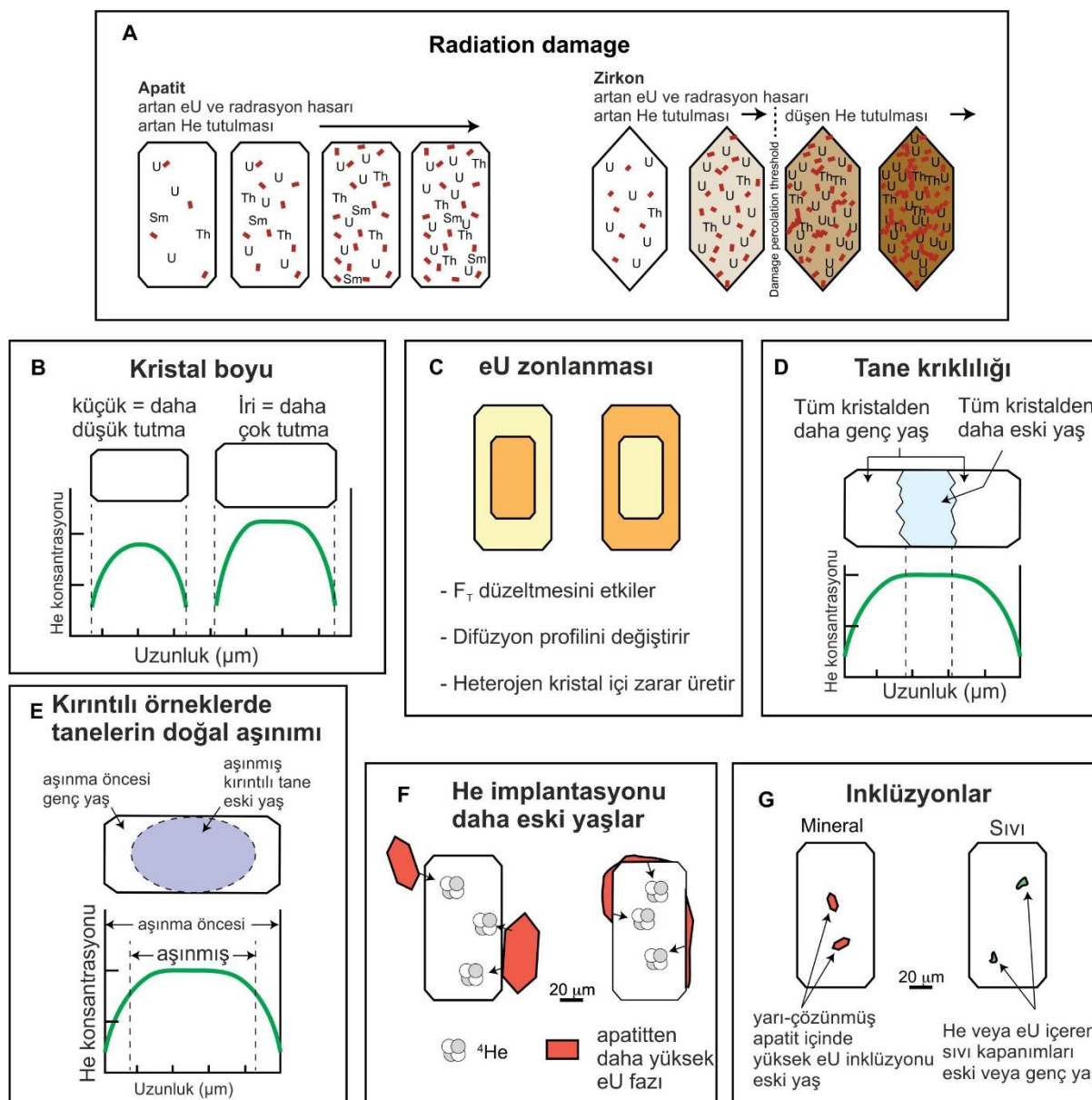
Buradan eU (efektif Uranyum) miktarı: $\text{U} + 0.24\text{Th}$ ve 0.0005Sm olarak hesaplanabilir. Görüldüğü üzere Sm yok sayılabilen mikarda He üretir, ancak sistemin içerdiği Sm miktarına bağlı olarak oluşacak He miktarı yaş verisine etki eder.

Apatit kristallerinde ^4He parçacıkları $\sim 40^\circ\text{C}$ altında tamamen tutulurlar, ancak $\sim 40^\circ\text{C}$ ile $\sim 70^\circ\text{C}$ arasında kısmen tutulurlar. $\sim 70^\circ\text{C}$ üstünde ise ^4He parçacıkları kristal kafesten salınırlar (Farley, 2000; Farley, 2002; Farley ve Stockli, 2002). Zirkon kristallerinde ise kapanma sıcaklığı $\sim 170\text{--}190^\circ\text{C}$ iken kısmi tutulma (Partial Retension Zone – PRZ) $\sim 130\text{--}180^\circ\text{C}$ arasındadır (Reiners vd., 2004; Reiners ve Brandon, 2006).

U-Th/He yönteminde analizleri etkileyen faktörleri göz önünde bulundurarak ölçümlerin yapılması gerekmektedir. Ölçümleri etkileyebilecek faktörler; kristal sistemleri içindeki raddrasyon hasarı, kristal boyutu, eU zonlanması, kristal kıırılılığı, kıırıntı kristallerde doğal aşınma, kenar taneden gelen He ve inklüzyonlardır.

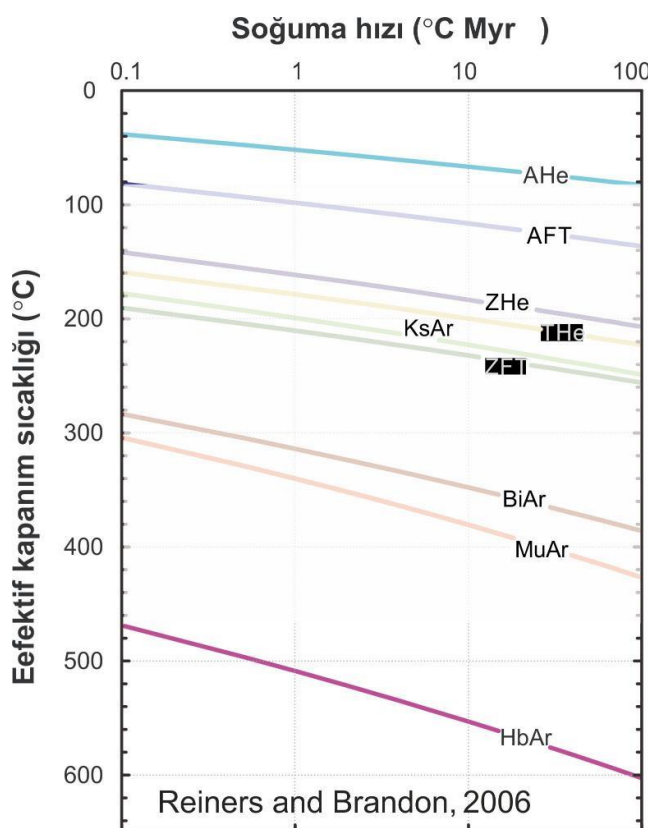
Kristaliçinde bulunan raddrasyon hasarı belli bir aşamaya kadar He tutulmasını artırırken, eşik değerin üstünde tutulmayı zayıflatarak He salınımını artırıcı etki eder. Kristal boyutu küçük olan tanelerde tutulma düşük olurken iri kristallerde tutulma daha fazla olur. Kristal içinde U, Th ve Sm dağılımı homojen olmaz ise eU zonlanması analizi olumsuz etkiler. Kıırık tanelerde

kristalin hangi parçasının ölçüldüğüne bağlı olarak orjinal yaştan küçük veya büyük yaşlar kesaplanabilir. Özellikle kırtıltılı tanelerde taşınma süreçlerine bağlı olarak krstaller kenarlarından itibaren aşınmaya maruz kalır ve He tutulması zayıflar. Komşu krstallerden (örn. Apatit kenarına zirkon) gelen He ölçümü yapılacak olan kristal içinde tutularak örneğin yaşıni yükseltici etki yapabilir. Son olarak kristal içinde mineral (ör. Apatit içinde zirkon) veya sıvı kapanımları örneğin He yaşına etki eder (Flowers vd. , 2022) (Şekil 7).



Şekil 7. U-Th-Sm/He yaşlarını etkileyen faktörler a) raddrasyon hasarının He salım kinetiğine etkisi, b) tane boyutunun He salım kinetiğine etkisi, c) eU zonlanması, d) tane kırıklılığı, e) kırtıltılı örneklerde tanelerin doğal aşınımı, f) zengin eU veya zengin eU tane kenarına sahip “kötü komşu”dan He implantasyonu ve g) mineral veya sıvı kapanımı (Flowers vd. , 2022)'den türkçeleştirilmiştir.

Burada FT ve He yöntemleri için efektif kapanma sıcaklıklarını verilmesine karşın mineral kristal sistemlerinin soğuma hızlarına bağlı olarak kapanma sıcaklıklarını değiştirmektedir (Reiners ve Brandon, 2006) (Şekil 8). Soğuma hızı düşük olan sistemlerin kapanma sıcaklıklarını soğuma hızı yüksek olan sistemlerden daha düşüktür. Örneğin Apatit Fizyon İzi $10^{\circ}\text{C}/\text{My}$ soğuma hızında kapanma sıcaklığı $110-120^{\circ}\text{C}$ iken $1^{\circ}\text{C}/\text{My}$ soğuma hızında kapanma sıcaklığı 90°C 'dir (Şekil 8).

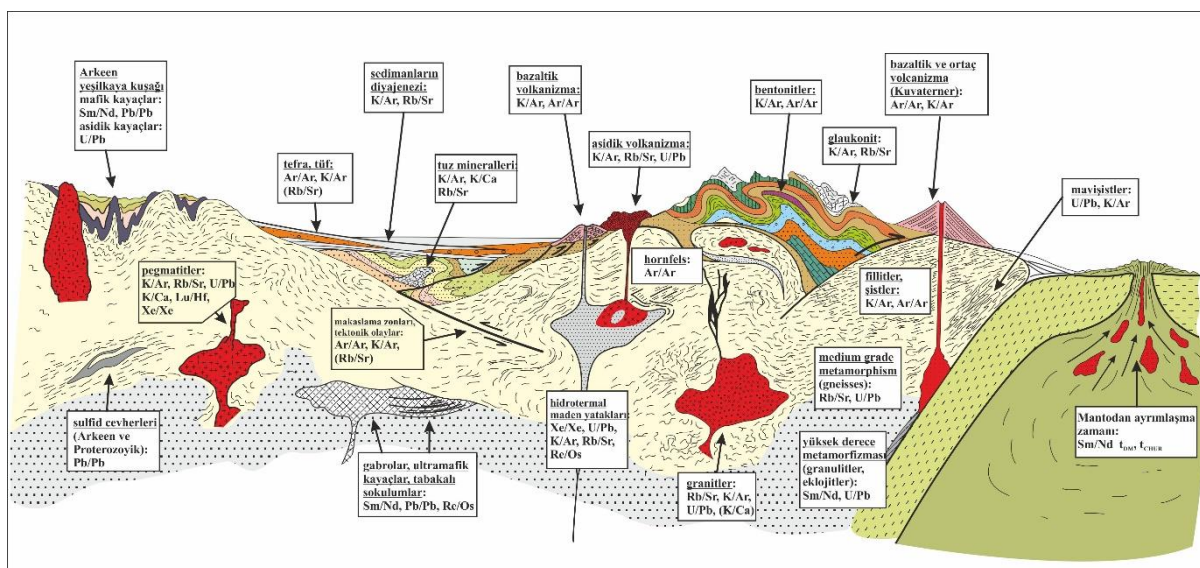


Şekil 8. Soğuma hızlarına bağlı olarak değişen kapanma sıcaklıkları (Reiners ve Brandon, 2006).

Düşük sıcaklık Temokronolojisini kullanım alanları

Jeokronoloji yöntemleri ile kayaçların/orneklerin formasyon/oluşum yaşı hesaplanırken, termokronoloji kapanma sıcaklıklarına bağlı soğuma yaşları hesaplanmaktadır (Şekil 9). Düşük sıcaklık termokronolojisi (LTT) ise kapanma sıcaklığı düşük olan ($<300-350^{\circ}\text{C}$) olan termokronoloji yöntemleridir. LTT genellikle üst kabuk hareketleri ve/veya mantonun üst kabuğa etkisi ile şekillenen jeolojik olayların zamanlaması ve hızının hesaplanması için kullanılır. Ancak LTT yöntemleri, hidrotermal ortamlar, volkanizma veya faylanma ile ilişkili alanlarda terminoloji olarak jeokronometre olarak kullanılabilir ve bu sistemlerin oluşum

zamanı hesaplanabilir (Reiners ve Ehlers, 2005; Dempster ve Persano, 2006; Reiners ve Brandon, 2006; Peyton ve Carrapa, 2013).

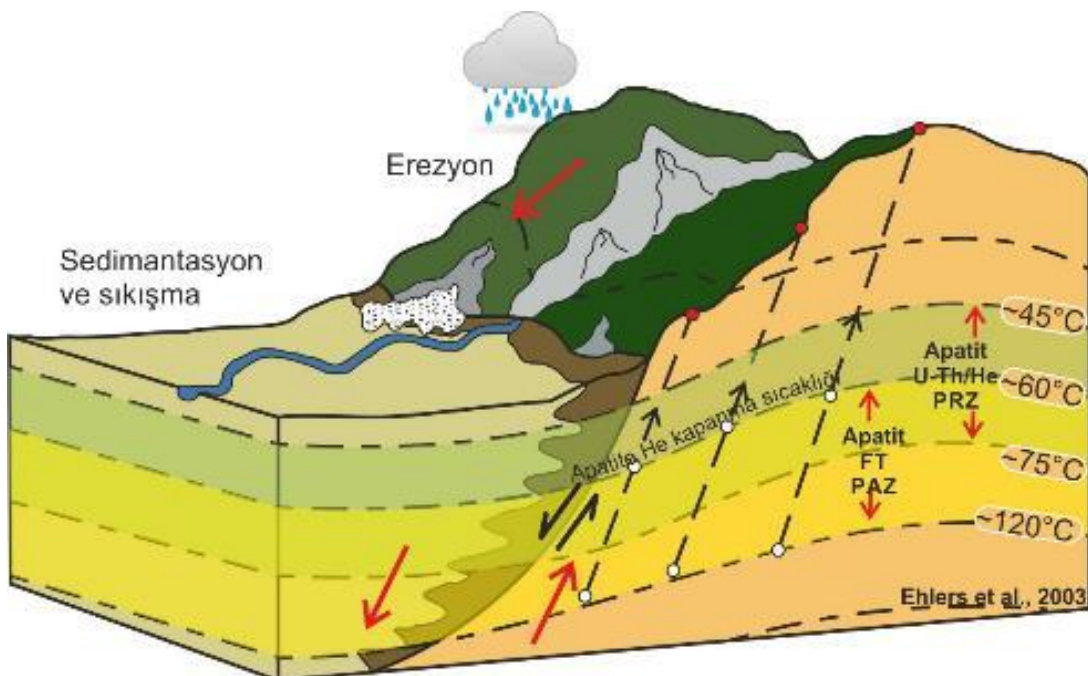


Şekil 9. Farklı jeolojik ortamlarda gerçekleştirilebilecek farklı jeo/terma-kronoloji yöntemleri (Geyh ve Schleicher, 1990).

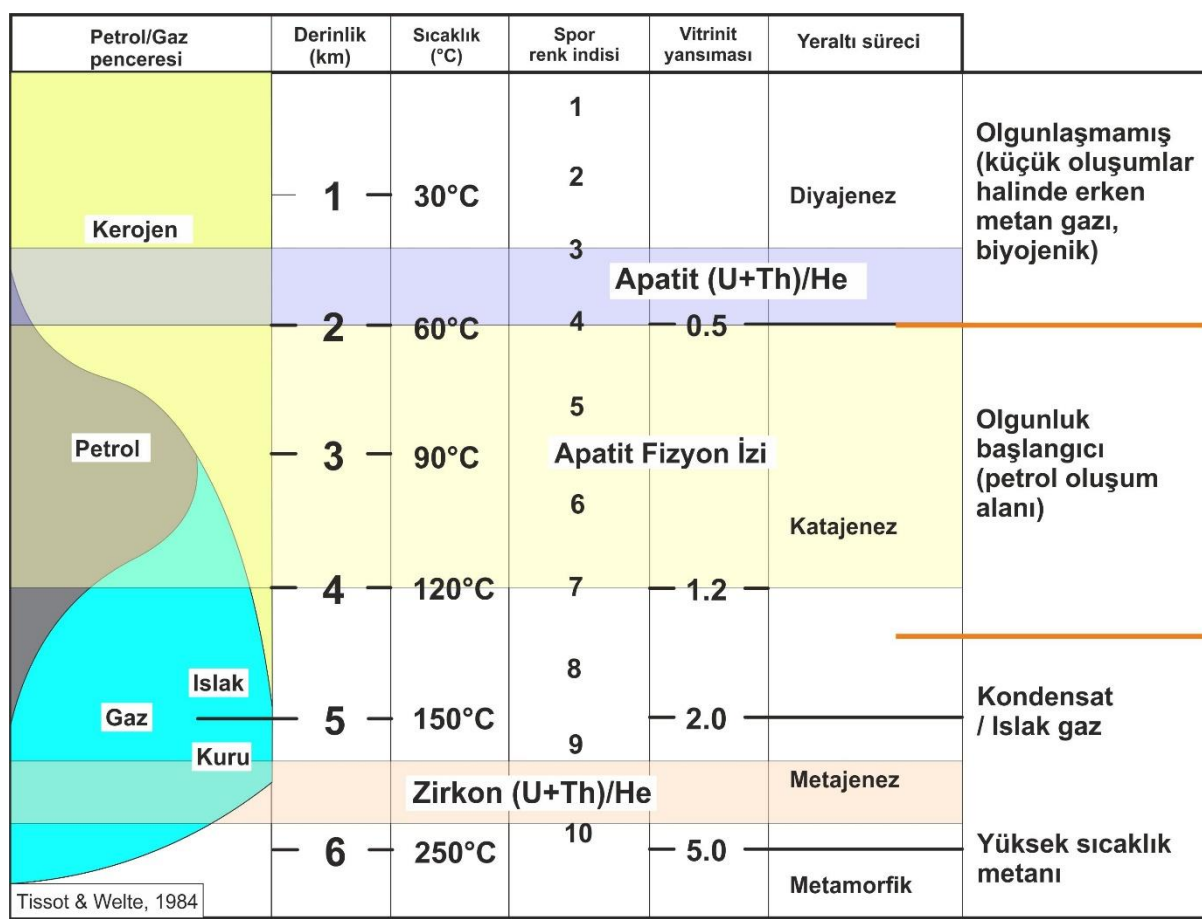
Kayaçlar yüzeye yaklaştıkça (yükseleme) veya erozyonal süreçler (aşınma, faylanması) ile mineral sistemlerinin kapanma sıcaklıklarına bağlı olarak LTT PAZ ve PRZ alanlarından yükselerek yüzeye yaklaşırlar (Şekil 10). LTT yönteminin en genel kullanımı yüksekliğe bağlı örneklemeye yaparak ana kayanın yükselme zamanı ve yükselim hızı hesaplanabilmektedir. Örneklerarası yükseklik farkı ve yaş farkından örneklerin kapanma sıcaklıklarına karşılık gelen derinliği geçiş zamanları ve yol-zaman oranları ile de yükselim hızı hesaplanabilir (Şekil 10). Burada en düşük LTT yaşı en altta en büyük LTT yaşı en üstte yer alır. Aynı yöntem bir üzerinde farklı LTT (ZFT, ZHe, AFT, AHe gibi) yöntemleri ve bunların kapanım sıcaklıklarına karşılık gelen derinlik farkından yükselim hızı hesaplanabilir (Şekil 10, 11). Bu tip anakayaların aşınma-taşınma ile havzalara taşınması ile buralarda depolan termokronometreler stratigrafik yaşlara göre sistematik örneklemeye ile kaynak alanın yükselme hızı ve erozyon hızı hesaplanabilir (Ehlers ve Farley, 2003; Reiners ve Ehlers, 2005; Reiners ve Brandon, 2006) (Şekil 10).

Sedimanter havzalarda hidrokarbon oluşumu için biriken orhanik materyalin olgunluğu kaynak alanın ve sedimanter havzanın en yüksek sıcaklığı ve termal tarihçesine bağlıdır. Sedimanter havzalarda devam eden beslenmeye bağlı gelişen gömülme ve tektonizmaya bağlı yüzeylemeler bu havzaların termal tarihçelerini karmaşık hale getirmektedir. LTT yöntemleri

ve bağımsız diğer değişkenler (vitrinit yansımıası, kayaç-evrimi vs.) kullanılarak havzanın zaman-sıcaklık ilişkisi ortaya çıkarılabilir (Tissot ve Welte, 1984; Peyton ve Carrapa, 2013; Schneider ve Issler, 2019) (Şekil 11).



Şekil 10. Normal faylanmalı alanlarda termal gradyanın hareketi ve AFT PAZ ve AHe PRZ alanları.



Şekil 11. Hidrokarbon oluşumu ve paleosıcaklık indisleri ile LTT ilişkisi (Tissot ve Welte, 1984).

REFERENCES

- Armstrong, P.A., 2005. Thermochronometers in Sedimentary Basins. Sayfa 499-525. Low-Temperature Thermochronology: Techniques, Interpretations, and Applications. Editör: Reiners, P.W., Ehlers, T.A. *Mineralogical Society of America*.
- Chew, D.M., Spikings, R.A. 2015. Geochronology and Thermochronology Using Apatite: Time and Temperature, Lower Crust to Surface. *Elements*, 11 (3), 189-194.
- Dempster, T.J., Persano, C. 2006. Low-temperature thermochronology: Resolving geotherm shapes or denudation histories?. *Geology*, 34 (2), 73-76.
- Donelick, R.A., O'Sullivan, P.B., Ketcham, R.A., 2005. Apatite Fission-Track Analysis. Sayfa 49-94. Low-Temperature Thermochronology: Techniques, Interpretations, and Applications. Editör: Reiners, P.W., Ehlers, T.A. *Mineralogical Society of America*.
- Ehlers, T.A., Farley, K.A. 2003. Apatite (U-Th)/He thermochronometry: methods and applications to problems in tectonic and surface processes. *Earth and Planetary Science Letters*, 206 (1-2), 1-14.

- Ehlers, T.A., 2005. Crustal Thermal Processes and the Interpretation of Thermochronometer Data. Sayfa 315-350. Low-Temperature Thermochronology: Techniques, Interpretations, and Applications. Editör: Reiners, P.W., Ehlers, T.A. *Mineralogical Society of America*.
- England, P., Molnar, P. 1990. Surface Uplift, Uplift of Rocks, and Exhumation of Rocks. *Geology*, 18 (12), 1173-1177.
- Enkelmann, E., Garver, J.I. 2016. Low-temperature thermochronology applied to ancient settings. *Journal of Geodynamics*, 93, 17-30.
- Farley, K.A. 2000. Helium diffusion from apatite: General behavior as illustrated by Durango fluorapatite. *Journal of Geophysical Research-Solid Earth*, 105 (B2), 2903-2914.
- Farley, K.A., 2002. (U-Th)/He Dating: Techniques, Calibrations, and Applications. Sayfa 819-844. Noble Gases in Geochemistry and Cosmochemistry. Editör: Porcelli, D.P., Ballentine, C.J., Wieler, R. *Reviews in Mineralogy and Geochemistry*.
- Farley, K.A., Stockli, D.F., 2002. (U-Th)/He Dating of Phosphates: Apatite, Monazite, and Xenotime. Sayfa 559-577. Phosphates. Editör: Kohn, M.L., Rakovan, J., Hughes, J.M. *Mineralogical Society of America*.
- Fleischer, R.L., Price, P.B., Walker, R.M. 1975. Nuclear tracks in solids: Principles and applications. Berkeley, USA: University of California Press.
- Flowers, R.M., Ketcham, R.A., Enkelmann, E., Gautheron, C., Reiners, P.W., Metcalf, J.R., Danišík, M., Stockli, D.F., Brown, R.W. 2022. (U-Th)/He chronology: Part 2. Considerations for evaluating, integrating, and interpreting conventional individual aliquot data. *GSA Bulletin*.
- Geyh, M.A., Schleicher, H. 1990. Absolute Age Determination: Physical and Chemical Dating Methods and Their Application. Berlin Heidelberg: *Springer Berlin Heidelberg*.
- Gleadow, A.J.W., Duddy, I.R., Green, P.F., Hegarty, K.A. 1986a. Fission-Track Lengths in the Apatite Annealing Zone and the Interpretation of Mixed Ages. *Earth and Planetary Science Letters*, 78 (2-3), 245-254.
- Gleadow, A.J.W., Duddy, I.R., Green, P.F., Lovering, J.F. 1986b. Confined fission track lengths in apatite: a diagnostic tool for thermal history analysis. *Contributions to Mineralogy and Petrology*, 94 (4), 405-415.
- Green, P.F., Duddy, I.R., Gleadow, A.J.W., Tingate, P.R., Laslett, G.M. 1986. Thermal Annealing of Fission Tracks in Apatite .1. A Qualitative Description. *Chemical Geology*, 59 (4), 237-253.
- Green, P.F., Duddy, I.R., Laslett, G.M., Hegarty, K.A., Gleadow, A.J.W., Lovering, J.F. 1989. Thermal Annealing of Fission Tracks in Apatite .4. Quantitative Modeling Techniques and Extension to Geological Timescales. *Chemical Geology*, 79 (2), 155-182.

- Hurford, A.J., 2019. An Historical Perspective on Fission-Track Thermochronology. Sayfa 3-23. Fission-Track Thermochronology and its Application to Geology. Editör: Malusà, M.G., Fitzgerald, P.G. Cham: *Springer International Publishing*.
- Ketcham, R.A., Donelick, R.A., Carlson, W.D. 1999. Variability of apatite fission-track annealing kinetics: III. Extrapolation to geological time scales. *American Mineralogist*, 84 (9), 1235-1255.
- Laslett, G.M., Green, P.F., Duddy, I.R., Gleadow, A.J.W. 1987. Thermal Annealing of Fission Tracks in Apatite .2. A Quantitative-Analysis. *Chemical Geology*, 65 (1), 1-13.
- Peyton, S.L., Carrapa, B., 2013. An introduction to low-temperature thermochronologic techniques, methodology, and applications. Sayfa 15-36. Application of structural methods to Rocky Mountain hydrocarbon exploration and development. Editör: Knight, C., Cuzella, *J.AAPG Studies in Geology*.
- Reiners, P.W., Spell, T.L., Nicolescu, S., Zanetti, K.A. 2004. Zircon (U-Th)/He thermochronometry: He diffusion and comparisons with $^{40}\text{Ar}/^{39}\text{Ar}$ dating. *Geochimica Et Cosmochimica Acta*, 68 (8), 1857-1887.
- Reiners, P.W., Ehlers, T.A. 2005. Low-Temperature Thermochronology: Techniques, Interpretations, and Applications. *Mineralogical Society of America*.
- Reiners, P.W., Brandon, M.T. 2006. Using thermochronology to understand orogenic erosion. *Annual Review of Earth and Planetary Sciences*, 34 (1), 419-466.
- Schneider, D.A., Issler, D.R., 2019. Application of Low-Temperature Thermochronology to Hydrocarbon Exploration. Sayfa 315-333. Fission-Track Thermochronology and its Application to Geology. Editör: Malusà, M.G., Fitzgerald, P.G. Cham: *Springer International Publishing*.
- Tagami, T., 2005. Zircon Fission-Track Thermochronology and Applications to Fault Studies. Sayfa 95-122. Low-Temperature Thermochronology: Techniques, Interpretations, and Applications. Editör: Reiners, P.W., Ehlers, T.A. *Mineralogical Society of America*.
- Tissot, B.P., Welte, D.H. 1984. Petroleum Formation and Occurrence. Heidelberg: *Springer*, Berlin.
- Wagner, G.A., Reimer, G.M. 1972. Fission track tectonics: The tectonic interpretation of fission track apatite ages. *Earth and Planetary Science Letters*, 14 (2), 263-268.
- Zaun, P.E., Wagner, G.A. 1985. Fission-track stability in zircons under geological conditions. *Nuclear Tracks and Radiation Measurements* (1982), 10 (3), 303-307.
- Zeitler, P.K., Herczeg, A.L., McDougall, I., Honda, M. 1987. U-Th-He Dating of Apatite - a Potential Thermochronometer. *Geochimica Et Cosmochimica Acta*, 51 (10), 2865-2868.

Laser Ablation Time of Flight Mass Spectrometry

Hamdi Şükür KILIÇ

Selcuk University, Faculty of Science, Department of Physics, 42031, Campus, Selcuklu, Konya, TÜRKİYE

Introduction

Spectroscopy is a technique which is the measurement of the response of Materials to energy in the case of interaction of energy with matter. During the interaction of energy with matter photoluminescence phenomena are taken place. **The photoluminescence phenomena includes the absorption and emission of light by matter in anyway.** A general interpretation of spectrometer by which spectroscopy job is executed is given in Figure 1.

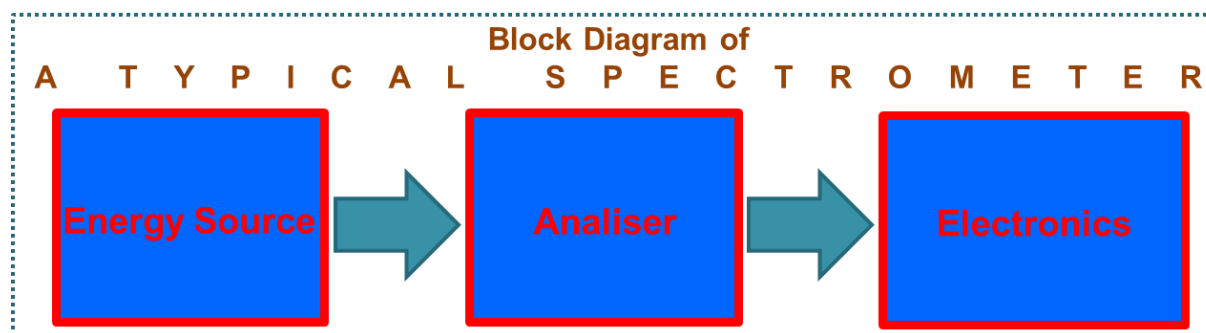


Figure 1 : A block diagram of a typical spectrometer

Spectrometer consists of three main components which can be described as **1)** source of energy, **2)** interaction room as an analiser/spectrometer and **3)** data acquisition system. In a general speaking; several form of energy may be used to investigate interaction of enegy with matter such as kinetic energy of accelerated fast particles, electrical arc, thermal energy or energy of electromanyetic waves (EMW).

As a spectroscopic technique, mass spectrometry has been used for this work and details of typical mass spectrometer also can be discussed in the view of these three part of a spectrometer to be;

- 1)** Source of Energy (fast particles, thermal, electric arc avd Electromegnetic waves),
- 2)** Analizer (several typer of spectrometers) (several types of mass spectrometers) (in our case, L-TOF-MS)
- 3)** Data Acquisition System (detectors, measuring electronics, oscilloscopes and computers)

Mass spectrometry is the most commonly used and very powerful/sensitive analytical apparatus, detects ionic samples and records spectra as a function of the **mass-to-charge ratio (m/z)** of atom or molecules exists in sample. Mass spectra obtained is used to identify, quantify unknown components of materials and to determine structure as well as chemical properties of molecules in terms of the **exact molecular weight** of the sample.

Mass spectrometer consists of three components of **(1) Ion Source**, **(2) Mass Analyzer** and **(3) Ion Detection System**, Let us discuss these three parts very briefly.

1) Ion Source

Mass spectrometry deals with ionic structure and measure ions. Sample introduction system in mass spectrometry has a key importance. In this technique, ions may be produced outside of spectrometer and introduce to analysis or it may be produced in the vacuum chamber which is called ionisation source. Therefore, before/after introduction the sample into mass spectrometer, atoms or molecules are converted to **gas-phase ions** and then they can be moved, accelerated or focused by several form of electrostatic lenses which create external electric and magnetic fields. In our laboratory, we have Linear Time of Flight Mass Spectrometer (L-TOF-MS) and Reflectron Time of Flight Mass Spectrometers (Re-TOF-MS) and used in connection to laser energy source to perform multiphoton ionisation process. Laser based ionisation technique allows us to obtain positively charged ions with removal of one or more electrons, depending on the experimental conditions as well as power and wavelength of laser beam.

Laser based ionisation technique allow us to have enough energy intensities. In our laser laboratories, we have several systems of nanosecond and femtosecond pulsed laser systems and these systems produce laser beam intensities at focal point are about $10^{8-12} W/cm^2$ for high power nanosecond laser system and $10^{8-15} W/cm^2$ for high power femtosecond laser system). Using these laser beam intensities with available output wavelengths, we can perform laser ablation and ionisation techniques to perform solid material analysis with mass spectrometry. The most commonlu applied ionisaton

Thermal Ionisation
Sparc souce
Electron Impact(EI)
Photoionisation (PI)
Chemical Ionisation (CI)
Field Ionisation (FI)
Field Desorption (FD)
Multiphoton ionisation (MPI)
Fast atom Bombardment (FAB)
Plasma desorption mass spectrometry (PDMS)
Secondary Ion Mass Spectrometry (SIMS)
Thermospray (TS)
Infrared laser desorption (IRLD)
Matrix Asisted Laser Desorption/Ionisation (MALDI)
Electrospray Ionisation (ESI)

Table 1: A list of ionisation techniques. Green coloured techniques can be applied in our laboratories.

techniques can be listed as in Table 1 where techniques are available in our laboratories are indicated in green colour.

In this study, we are going to give a brief description of laser based ionisation techniques available and applicable in our studies.

One of the most commonly used ionisation techniques after invention of lasers are photo ionisation technique in which instead of electrons, photons from available laser which produce photons over very large range of spectrum are used for apply a single or multiphoton excitation and ionisation process with usage of enough energy absorbed to produce positive ions with removal of one or more electrons in a gas or vapour sample.

In the most common laser, a fixed fundamental output wavelength but a limited tunable sources of laser output are also available and wavelength of laser beam can be tuned over a number of resonance transitions of samples. In order to obtain somehow higher elemental selectivity, resonance ionization techniques may be applied for selectivity.

2) The Mass Analyzer

Several types of mass analysers are currently in use world wide and available commercially. Each of mass analysers has different properties as well as performances based on speed of operation, resolution and sensitivities. The types of mass analysers may be listed as in Table 2.

The instruments used in **Mass spectrometry** are called mass spectrometers and they operate on the principle of detecting ions and ions may be controlled and manipulated by electric/magnetic fields and focused on the detector to be electrically detected by critical detectors.

Mass spectrometers have five main components: a sample inlet system, an ion source, an analyzer and a detector all in a vacuum chamber and data acquisition system. Energy source and data acquisition system other than detector may be located outside of the vacuum chamber. Inlet system: is designed to introduce sample to the spectrometer in either ionic or neutral forms, either gas phase or liquid phase of sample. In the case of liquid sample, it is introduced into

Mass Analysers
Magnetic Sector (B)
Double-focusing (EB)
Reverse Geometry (BE)
Ion cyclotron resonance (ICR)
Quadrupole (Q)
Quadrupole Ion Trap (QITMS)
Radio Frequency (RF)
Time of Flight (TOF) MS
Reflectron Time of Flight MS
Fourier transform (FTMS)
Triple Quadrupole (QQQ)
Four Sector (EBEB)
Hybrid (EBQQ)
Hybrid (EB-TOF)
Tandem TOF-TOF
Laser Ablation ICP MS

Table 2: A list of analysers in different design.

vacuum condition in spectrometers, samples expands into vacuum and expanda in the gas form and the analised. If sample is in the solide form, it can be evaporated through laser ablation proveress and than after sample becomes vapor of neutrals, it can be hited by extra laser beam in same pulse or second pulse comes from another laser. After these process are taken place, ions of samples are obtaine within volume of laser pulses and the ions are detected by the detectors.

3) Ion Detection System

After production of ions, they are send to detector by separating them by analysier and then measured by detector. They are measured by tedector and then send to data acquisitions system where data are saved into a digital environment as a function of m/z ratio in their relative abundance. Therefore, a **mass spectrum** is simply produced as a function of m/z ratios of the ions present in a sample and a graph of the ion intensities at a special m/z ration is plotted against their relevant m/z ratio. Each peak in a mass spectrum shows a component of unique m/z in the sample, and heights of the peaks connote the relative abundance of the various components in the sample.

In the case of our aparatuses which are TOF-MS spectrometer, ion intensities are measured as function of Time of Flight of ions. In this case, the lihtest ion reaches at detector at the shortest time while the heaviest ion is the last. The ions have m/z masses between the lihghest and heaviest reach at bdetector between the shortes time for the lightest ion and the longest time fort he heaviest ion reached. Therefore, ions with m/z ration feom smallest m/z ratio to the largest one can be measured as a function TOF which is the time consumed by ions from the time at which produced to the time at which they reaches at detector. So, the spectrum is produced as a function TOF and ion intensities are plotted versus TOF of each ion as shown in Figure 3.

Investigation of many samples have been carried out and measured to determine unnown components of samples and characterised them by mass spectrometers. Doing this type analysis, these investigations can be performed to identify as well as distinguish the isotopes of chemical elements and determine their masses and abundances, analysis the geologic samples,

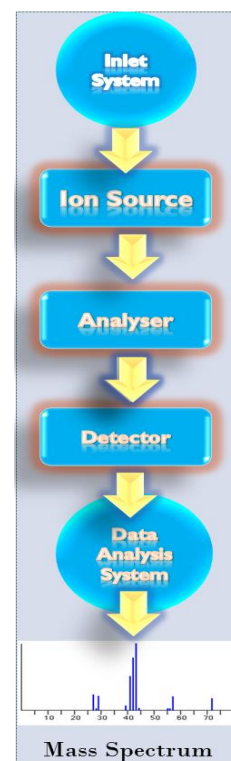


Figure 2: Components of a typical mass spectrometer.

inorganic and organic chemicals, determine the structural formula of complex organic substances, the strengths of chemical bonds and energies necessary to produce particular ions.

Electronics

The operation of a mass spectrometer and measurement of signals depend on technique and suitable electronics used. These electronics are chosen due to what is to be measured and which properties of Materials interested in. In the mass spectrometry, ions or amounts of ionic samples are needed to be measured. In order to measure ionic samples, power supplies are required to supply either extraction optics in the ion source or detectors. These power supplies have to be able to give outputs as stable as obtaining stable ion signal measured by detector.

Detectors
Photographic plate
<u>Faraday Cup</u>
<u>Electron multiplier</u>
Magnetic electron multiplier
Continous dynode multiplier
<u>Continous dynode multiplier</u>
Dual channel plate
Daly detector
Diod array detector
Image current
Inductive detector

Table 3: A list of detectors available commercially and may be used to detect ions in mass spectrometers in different design.

Presentation of A Typical TOF Mass Spectrum

In our laboratories, we have L-TOF-MS and Re-TOF-MS systems. Therefore, I am going to give a typical mass spectrum taken using a L-TOF-MS system. As I indicated before, in TOF-MS system, all information about sample can be obtained together in a TOF mass spectrum within a laser pulse time duration. All data with all ion peaks exists in sample can be recorded simultaneously. A typical L-TOF mass spectrum is shown in Figure 3. Data was taken from methane sample as an example to present here.

A typical time of flight mass spectrum is shown in Figure 3. Spectrum shows relative intensities of fragment ions of C^+ at m/z 12, CH^+ at m/z 13, CH_2^+ at m/z 14, CH_3^+ at m/z 15 and CH_4^+ at

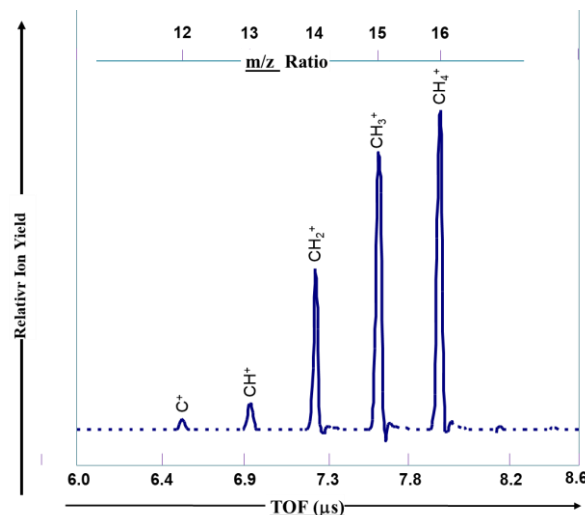


Figure 3: A typical mass spectrum of time of flight (TOF) is presented, taken by using a L-TOF-Mass Spectrometer

m/z 16 which reached at detector at 6.5 μ s, 6.9 μ s, 7.2 μ s, 7.6 μ s and 8.0 μ s, respectively. Figure shows m/z ratios for ions at upper axis while TOF at lower axis in horizontal axes. Vertical axis of graph shows relative intensities of ion peaks in arbitrary units. As can be seen from spectrum, the lightest mass reaches at detector the first and the largest mas reaches at detector the latest and spectrum is recorded as a function of time of flight and called time of flight mass spectrum.

Elektron Mikroprob ile Yaşılandırma Tekniği

Kıymet DENİZ^{1,2}

¹*Ankara Üniversitesi, Mühendislik Fakültesi, Jeoloji Mühendisliği Bölümü, Ankara/TÜRKİYE*

²*Ankara Üniversitesi Yerbilimleri Uygulama ve Araştırma Merkezi (YEBİM), Ankara/TÜRKİYE
kdeniz@eng.ankara.edu.tr*

Öz

Yerkabuğunun oluşumu, magmatik, metamorfik, sedimanter kaya birliliklerinin oluşumu veya metalojenik süreçler gibi jeolojik araştırmalarda doğru jeokronoloji çok önemlidir. Dolayısıyla görelî yaşılandırma tekniklerinin yetersiz kalması ve mutlak yaşılandırma ile radyometrik yaşılandırma tekniklerinin gelişimi ile yüksek hassasiyette doğru analitik yaşı verilerinin eldesi mümkün olmuştur. Elektron Prob Mikro Analiz (EPMA) odaklanmış elektron demetinin bir numunenin yüzeyine gönderilip o yüzeyden görüntü, kimyasal analiz ve U-Th-Pb yaşılarının elde edilmesini sağlayan bir çeşit elektron mikroskopudur. EPMA, 1958'den beri jeolojik numunelerin kimyasal analizi için kullanılmaktadır. 1977 yılından itibaren kimyasal yaşılandırma için uygulanmaya başlanmıştır. EPMA tahribatsız, yerinde, yüksek çözünürlüklü, kolay erişilebilir ve uygulanabilir bir yaşılandırma yöntemidir. Yaşlar, U-Th mineralleri için μm ölçüğünde, ya doğrudan ince kesitler üzerinde ya da yüzeyi parlatılmış epoksiye alınmış mineral taneleri üzerinden hesaplanabilir. Uraninit, monazit, ksenotim, zirkon, badeleyit, torit, torianit, huttonit, keralit, brabantit, apatit gibi U ve Th içeriği yüksek mineraller kimyasal yaşılandırma için uygundur. EPMA ile kimyasal yaşılandırmaya uraninit ile başlanmış fakat monazitte yaygın olarak kullanılmaktadır. Monazit düşük Pb içeriği, çeşitli kaya türlerinde yaygın olarak bulunması, son derece değişken bileşimi nedeniyle ana kaya koşullarını yansıtması ve önceki jeolojik süreçleri kaydetmesi nedeniyle tercih edilmektedir. Kesin ve doğru veriler için numune hazırlama, detaylı kimyasal haritalama ve ölçüm koşulları çok önemlidir. Pb içermeyen numune hazırlaması esastır. U, Th, Pb ve Y'nin hızlanması gerilimi, prob akımı, işin çapı, pik ve arka plan sayma süreleri gibi ölçüm koşulları yaşılandırmada kullanılan minerale göre değişmektedir. Araştırmacılar, en iyi sonuçları elde etmek için farklı minerallerde farklı analitik teknikler uygulamışlardır. Tüm mineraller için önerilen işin çapı 1 μm 'dir. Monazit için önerilen hızlanması voltajı ve prob akımı sırasıyla 15 kV ve 100 nA'dır. U ve Pb'nin pik ve arka plan sayım süresi için önerilen en uygun ölçüm koşulları 200 ve 100 s iken Th ve Y'nin pik ve arka plan sayım süresi 100 ve 50 s'dir. Torit ve torianit için önerilen hızlanması voltajı, prob akımı ve U, Pb, Th ve Y'nin pik ve arka plan sayım süresi sırasıyla 20 kV, 100 nA ve 200 s'dir.

Ksenotim ölçümleri için genellikle U, Pb, Th ve Y'nin 30 kV hızlandırma gerilimi, 200 nA prob akımı ve 400 s pik ve arka plan sayma süreleri kullanılır. Zirkon ve badelleyit için 20 kV hızlandırma voltajı ile aynı prob akımı, pik ve arka plan sayma süresi kullanılır. Belirtilen yaşı hassasiyeti yaklaşık olarak 7-30 My arasındadır ve şartlara bağlı olarak değişim mümkündür. EPMA, mineral içindeki ayrıntılı bileşim değişikliklerini karakterize etmek, her alanın bileşimini analiz etmek ve 1 μm genişliğindeki her alanın yaşıını belirlemek için kullanılabilir. Kimyasal tarihlemenin ana avantajı, ID-TIMS, LA-ICP-MS, SIMS ve SHRIMP gibi izotopik tarihleme yöntemlerine göre nokta boyutudur. EPMA, kimyasal zonlama yapan ve birden fazla jeolojik süreci kaydeden mineraller için çok kullanışlı bir yaşlandırma tekniğidir. 100 My'dan eski kayaçlar tarihleme için daha uygundur, ancak 50 My'dan daha genç kayalar için de uygulanmaktadır. EPMA ile kimyasal yaşlandırma diğer tekniklere göre nispeten daha ucuzdur.

Anahtar Kelimeler: Elektron Mikroprob, kimyasal yaşlandırma, U-Th-U, monazit.

Dating Methods by using Electron Microprobe

Kıymet DENİZ^{1,2}

¹*Ankara University, Faculty of Engineering, Department of Geological Engineering, Ankara/TÜRKİYE*

²*Earth Sciences Application and Research Center (YEBİM) of Ankara University, Ankara/TÜRKİYE*

kdeniz@eng.ankara.edu.tr

Abstract

Accurate geochronology is very important in geological investigations such as the formation of the earth's crust, the formation of igneous, metamorphic, sedimentary rock associations or metallogenetic processes. Therefore, with the inadequacy of relative dating techniques and the development of absolute dating and radiometric dating techniques, it has become possible to obtain accurate analytical age data with high sensitivity. An Electron Probe Micro Analyzer (EPMA) is a kind of electron microscope, which allows a focused electron beam to be sent to the surface of a sample to obtain images, chemical analysis and U-Th-Pb dating from that surface. The EPMA has been used since 1958 for the chemical analysis of geological samples. It has been started to applicable for the chemical dating since 1977. The EPMA is a non-destructive, in-situ, high resolution, and easy accessible and applicable dating method. The ages can be calculated for U-Th minerals at μm scale, either directly on thin sections or on separated grains mounted in polished sections. The minerals which have high U and Th content such as uraninite, monazite, xenotime, zircon, badelleyite, thorite, thorianite, huttonite, cheralite, brabantite, apatite are appropriate for the chemical dating. The chemical dating via EPMA started with the uraninite and is widely applied to monazite. The monazite is preferred for its low common Pb content, existing widely in various types of rock, reflecting host rock conditions because of its extremely variable composition and recording the previous geological processes. The sample preparation, detailed chemical mapping and measurement conditions are very important for the precise and accurate data. The Pb free sample preparation is essential. The measurement conditions such as accelerating voltage, probe current, beam diameter, peak and background counting time of the U, Th, Pb and Y vary according to the mineral which are used for the dating. The researchers carried on different analytical techniques in different minerals for obtaining the best results. The suggested beam diameter is 1 μm for all minerals. The suggested accelerating voltage and probe current for the monazite are 15 kV and 100 nA, respectively. The suggested optimal measurement conditions for the peak and background counting time of U and Pb are 200 and 100 s whereas the peak and background counting time

of Th and Y are 100 and 50 s. The recommended accelerating voltage, probe current and the peak and background counting time of U, Pb, Th and Y for the thorite and thorianite are 20 kV, 100 nA and 200 s, respectively. The 30 kV accelerating voltage, 200 nA probe current and 400 s peak and background counting time of U, Pb, Th and Y are generally used for the xenotime measurements. The 20 kV accelerating voltage and the same probe current and peak and background counting time are used for the zircon and badelleyite. The stated age precision is approximately between 7-30 Ma and it depends the conditions. The EPMA can be used to characterize the detailed compositional changes within the mineral, analyze the composition of each domain and determine the age for each domain less than 1 μm in width. The main advantage of the chemical dating is spot size with respect to the isotopic dating methods such as ID-TIMS, LA-ICP-MS, SIMS and SHRIMP. The EPMA is very useful dating technique for the minerals which are chemical zoning and record the more than one geological processes. The rocks older than 100 Ma is more suitable for the dating however, it is also applicable for the rocks, which are younger than 50 Ma. The chemical dating with EPMA is relatively cheap according to the other dating methods.

Keywords: *Electron microprobe, chemical dating, U-Th-Pb, monazite.*

U-Pb Carbonate Dating Applications Using LA-ICP-MS

Gönenç Göçmengil

Istanbul Metropolitan Municipality, Department of Survey and Projects, Kasımpaşa, İstanbul, Turkey

gonencgocmengil@gmail.com

Abstract

LA-ICP-MS U-Pb carbonate becomes a powerful tool in the last 10 years since the emerging of the new analytical instruments, new measurement methods and new reference materials to the research area. Regarding the other techniques such as ID-TIMS, TIMS and IRMS, LA-ICP-MS systems needs much smaller volume of samples, acquired data much faster, and it is a much effective technique to differentiate different carbonate generation events.

Despite the aliquot-based techniques still the best ones in terms to acquire the lowest error range possible, emerging of the new reference materials to the field, and development of the analytical capabilities of the mass spectrometers improve the capabilities of the LA-ICP-MS instruments. In terms of different carbonate phases such as calcite, dolomite and aragonite, U-Pb calcite dating became much routinely handled and it is used to assess the many different geological problems such as brittle faulting, diagenesis, hydrocarbon migration, ore genesis, speleothem dating and many other different environments that bears calcite.

Even though the calcite LA-ICP-MS U-Pb dating display great improvements in the last decade, there are still many pitfalls including the homogeneity of the reference materials, behaviour of the U in carbonate series and homogeneity of the investigated samples themselves. Despite those problems, LA-ICP-MS U-Pb calcite dating is the most robust technique comparing to the other carbonate dating efforts.

Dolomite and aragonite LA-ICP-MS U-Pb dating efforts are still under investigation and different studies on dolomite dating gave much reliable results. On the other hand, aragonite minerals seem to display effected quite different to the ablation relative to calcite and dolomite. Therefore, the studies on those two minerals still lack suitable reference materials and much accurate methods.

Keywords: *geochronology, laser ablation, carbonate dating, method development*

1. Introduction

LA-ICP-MS U-Pb carbonate dating became an emerging field in the last decade by the incorporation of new reference materials, new instrumental techniques to resolve different problems such as brittle faulting, diagenesis, ore genesis, cave studies and many different environments that bearing carbonate (Li et al., 2014; Roberts & Walker, 2016; Nuriel et al., 2019; Burisch et al., 2019; Woodhead & Petrus, 2019; Roberts et al., 2020).

Even though the aliquot-based techniques such as ID-TIMS, TIMS, IRMS routinely used to extract the U-Pb ages from the different carbonate phases, incorporation of LA-ICP-MS instruments to conduct the age determination such as Liu et al (2014) and Roberts et al., (2016) getting attention in the field in last years.

Since the incorporation of the reference materials on calcite minerals (e.g. Roberts et al., 2017), various different topics have been investigated using calcite based LA-ICP-MS U-Pb dating. Since there is lack of reference materials and homogeneity problems for dolomite and aragonite phases (Guillong et al., 2020; Elisha et al., 2021), the following description only focused on calcite minerals and calcite dating.

There are couple of key points while doing LA-ICP-MS U-Pb carbonate dating before the measurement took place in the LA-ICP-MS instruments which will be explained below.

2. Fundamentals and problems of LA-ICP-MS carbonate U-PB dating technique

Since the calcites precipitated in different environments and their initial Pb values are different, interpretation of the data handled in two steps

- Correction of $^{207}\text{Pb}/^{206}\text{Pb}$ ratio using a homogenous reference material (usually handled using homogenous glass – NIST)
- U-Pb fraction determined and corrected using the lower intercept point by using matrix matched reference material (Guillong et al., 2020)

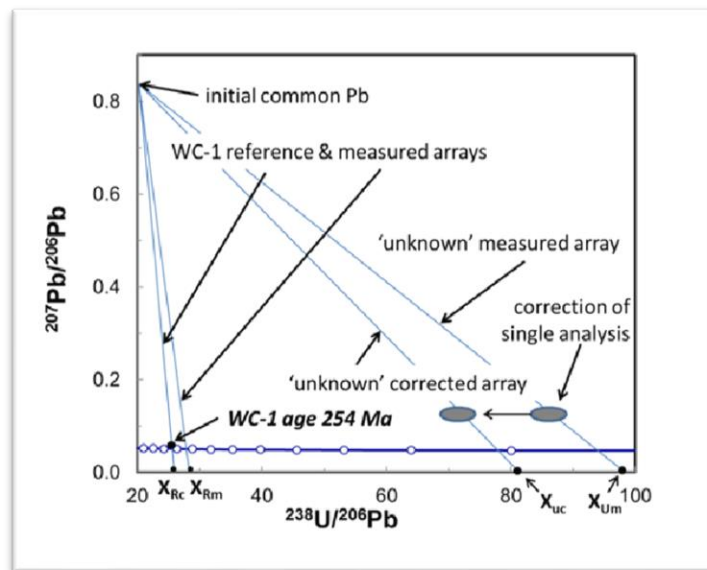


Figure 1. Tera- Wasserburg concordia diagram that show the calculation scheme of the calcite LA-ICP-MS data. Figure directly taken from Roberts, (2022).

An ideal U-Pb chronometer requires sufficient $^{238}\text{U}/^{204}\text{Pb}$ values or “ μ ”, relatively single age population. Apart from these, every analysis ideally corresponding to a “closed system, every analysis represented by similar initial Pb value. And if everything works well the MSWD value should be around 1 (Wendt and Carl, 1991).

However, the calcite systems and behavior of U and Pb in carbonates controlled by various factors such as partition coefficients, pH, eH and $p\text{ CO}_2$, Ca^+ and CO_2 ion sizes together with diffusion and open system problems. During the interpretation of the analysis, open system behavior must be carefully determined, otherwise strange results can be obtained using scattered data in Tera- Wasserburg space (Figure 2).

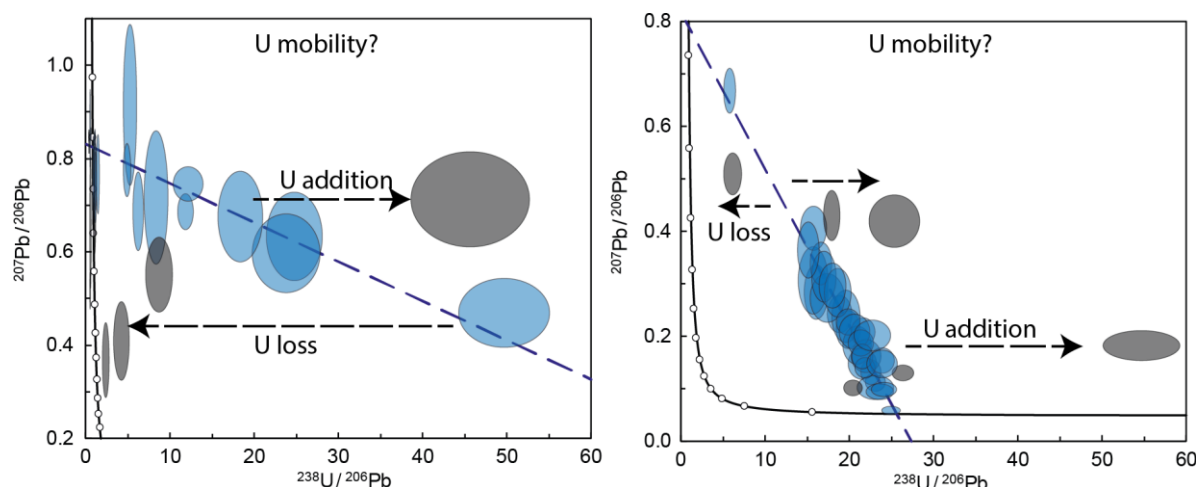


Figure 2. Tera- Wasserburg concordia diagram that show open systems behaviors (Roberts et al., 2020).

One of the other important factor to acquire the LA-ICP-MS U-Pb calcite ages is the inhomogeneties of the reference materials. Currently most used reference material named as WC-1 and described in Roberts et al., (2017). However, as pointed out by Guillong et al (2020), the inhomogeneities within the reference material itself can be problematic too since some portion of the WC-1 dated as nearly 200 Ma. (Figure 3).

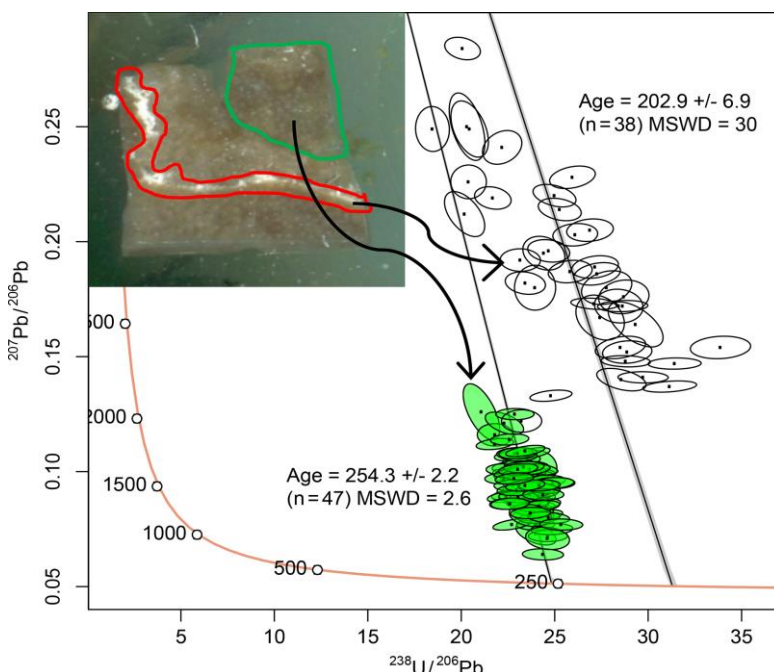


Figure 3. Tera- Wasserburg plot of the aliquot dating of the different portions of the WC1. The whitish portion of the sample gave quite lower age range, respect to the well-known age of the WC1 (around 250 Ma). (Directly taken from Guillong et al., 2020).

Even though the reference materials are problematic, emerging of the new ones such as JT (Guillong et al., 2020) and ASH-15D (Nuriel et al., 2020) and many new natural and synthetic materials (Boer et al., 2022) can give much precise results dating studies in the near future. Apart from these fundamental dating issues, directly dating of the carbonate phases by using image techniques became the fundamental tool to extract the crystallization conditions of the desired sample.

3. LA-ICP-MS U-Pb calcite dating using image based techniques

Like any other U-Pb dating applications, petrographic characterization of the desired sample must be thoroughly handled before analysis. To handle this issue, classical optical microscopy, SEM, cathodoluminescence, back-scattered electrons and rarely used techniques such as digital autoradiography conducted before analysis as explained by Roberts et al., (2020). Even though

these techniques are not directly sampled the U-rich zones within the sample, digital autoradiography technique can be used to assess the U rich portions without given sample any harm (Figure 4, Roberts et al., 2020).

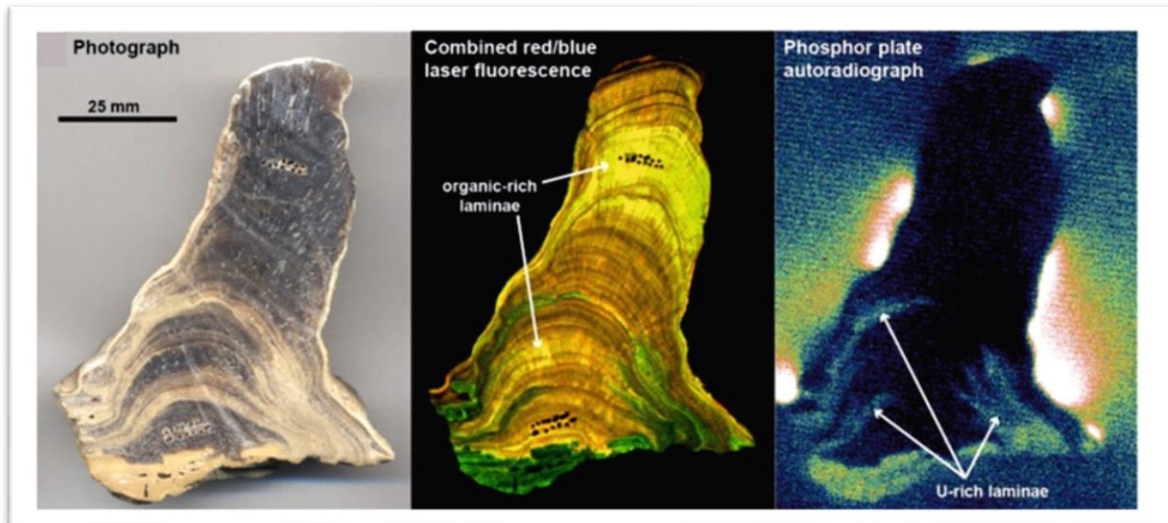


Figure 4. Detection of the U-rich portions using digital autoradiography (Figure taken from Roberts et al., 2020).

Apart from the non-destructive imaging techniques, the destructive ones are currently used as a direct tool to detect the U-Pb ages using calcite. As pointed out by Drost et al (2018), by pooling of pixels from 2d LA-ICP-MS elemental and isotopic data from the desired regions, different U rich regions can be dated in an accurate manner. Particularly Monocle add-on for Iolite software is frequently used to assess the ages (Figure 5).

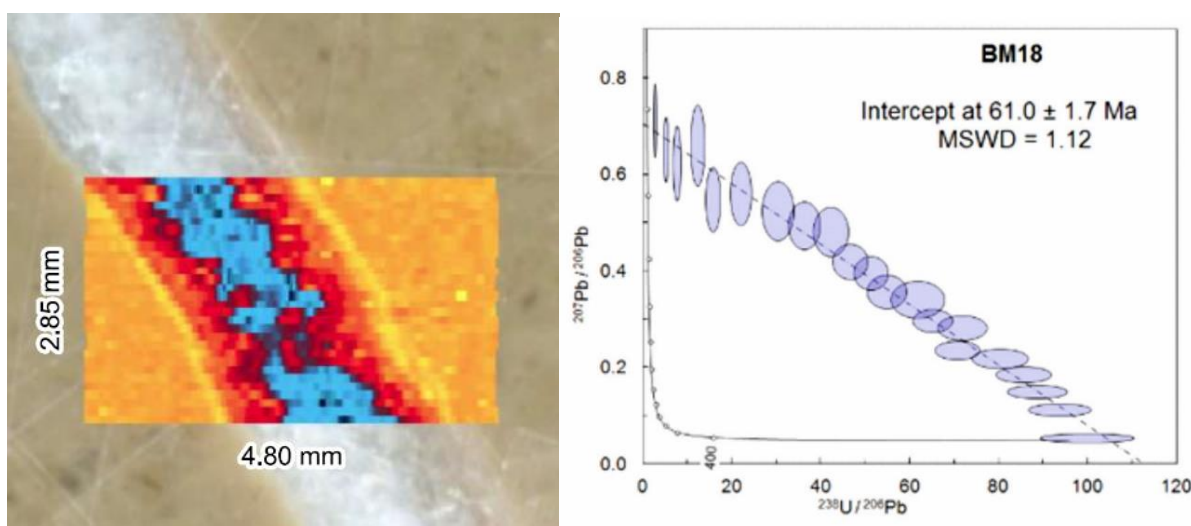


Figure 5. LA-ICP-MS ages extracted from a vein sample using Monocle ad inn of Iolite, the blue parts at the left hand side of the sample selected fro interpretaion. At the right side, ages of the blue parts given.

Conclusions

LA-ICP-MS U-Pb carbonate dating becomes a powerful tool to solve many geological problems, despite the limitation's calcite dating possibly going to be a routine tool to assess the many problems. On the other hand, dolomite and aragonite have the potential for U-Pb dating but there is great need for new studies to assess their suitability for dating.

REFERENCES

- Boer, W., Nordstad, S., Weber, M., Mertz-Kraus, R., Hönnisch, B., Bijma, J., & Reichart, G. J. (2022). A new calcium carbonate nano-particulate pressed powder pellet (NFHS-2-NP) for LA-ICP-OES, LA-(MC)-ICP-MS and μ XRF. *Geostandards and Geoanalytical Research*.
- Burisch, M., Gerdes, A., Meinert, L. D., Albert, R., Seifert, T., Gutzmer, J. 2019. The essence of time-fertile skarn formation in the Variscan Orogenic Belt. *Earth and Planetary Science Letters*, 519, 165-170.
- Drost, K., Chew, D., Petrus, J. A., Scholze, F., Woodhead, J. D., Schneider, J. W., Harper, D. A. 2018. An Image Mapping Approach to U-Pb LA-ICP-MS Carbonate Dating and Applications to Direct Dating of Carbonate Sedimentation. *Geochemistry, Geophysics, Geosystems*, 19(12), 4631-4648.
- Elisha, B., Nuriel, P., Kylander-Clark, A., Weinberger, R. 2020. Towards in-situ U-Pb dating of dolomites. *Geochronology Discussions*, 1-17.
- Guillong, M., Wotzlaw, J. F., Looser, N., Laurent, O. 2020. Evaluating the reliability of U-Pb laser ablation inductively coupled plasma mass spectrometry (LA-ICP-MS) carbonate geochronology: matrix issues and a potential calcite validation reference material. *Geochronology*, 2(1), 155-167.
- Li, Q., Parrish, R. R., Horstwood, M. S. A., McArthur, J. M. 2014. U-Pb dating of cements in Mesozoic ammonites. *Chemical Geology*, 376, 76-83.
- Nuriel, P., Craddock, J., Kylander-Clark, A. R., Uysal, I. T., Karabacak, V., Dirik, R. K., Weinberger, R. 2019. Reactivation history of the North Anatolian fault zone based on calcite age-strain analyses. *Geology*, 47(5), 465-469.
- Roberts, N. M., Walker, R. J. 2016. U-Pb geochronology of calcite-mineralized faults: Absolute timing of rift-related fault events on the northeast Atlantic margin. *Geology*, 44(7), 531-534.
- Roberts, N. M., Rasbury, E. T., Parrish, R. R., Smith, C. J., Horstwood, M. S., & Condon, D. J. 2017. A calcite reference material for LA-ICP-MS U-Pb geochronology. *Geochemistry, Geophysics, Geosystems*, 18(7), 2807-2814.

- Roberts, N., Drost, K., Horstwood, M., Condon, D., Drake, H., Milodowski, A., Imber, J. 2020. LA-ICP-MS U-Pb carbonate geochronology: strategies, progress, and application to fracture-fill calcite. *Geochronology Discussion*.
- Roberts, N. 2022. IGG-CAS Seminar: Carbonate LA-ICP-MS U-Pb geochronology (<http://dx.doi.org/10.13140/RG.2.2.20429.31203>).
- Wendt, I., & Carl, C. 1991. The statistical distribution of the mean squared weighted deviation. *Chemical Geology: Isotope Geoscience Section*, 86(4), 275-285.
- Woodhead, J., Petrus, J. 2019. Exploring the advantages and limitations of in situ U-Pb carbonate geochronology using speleothems. *Geochronology*, 1(1), 69-84.

The First U-Pb Zircon Geochronology Data of Karapınar Karacadağ Volcanics and Volcanostratigraphic Evolution of the Region

***Gülin Gençoğlu Korkmaz, Hüseyin Kurt & Kürşad Asan**

**Konya Technical University, Faculty of Engineering and Natural Sciences Department
of Geological Engineering, Selçuklu, Konya, Turkey**

***ggkorkmaz@ktun.edu.tr; ORCID NO: 0000-0003-0185-2806**

Abstract

The Karacadağ stratovolcano having a complex story is one of the significant volcanos within the Cappadocian Volcanic Province, located in Central Anatolia, Turkey. From the Late Miocene to Pliocene, it is outcropped as lava flows, dykes, sills and domes with the composition of dominantly andesitic-dacitic, and rarely basaltic-trachytic. However, Karapınar Volcanic Field (KPVF) contains Quaternary aged enclave bearing basalts, rarely andesites, dacites, trachy-andesites and their pyroclastics-maar pyroclastics. Here we report the volcano-stratigraphy, petrography and the preliminary U-Pb ages of the Karacadağ Volcanic Complex and Karapınar Volcanic Field.

1. Introduction

Mt. Karacadağ (Karapınar-Emirgazi Area) is one of the largest composite volcano in the Anatolia. In an attempt to establish a robust geochronological framework for this important volcanic field, we performed the first zircon U-Pb dating from the andesites and made stratigraphic sections to understand the volcanolgy and to interpret the importance of the area. Investigated volcanic rocks cover large areas from Karapınar to Emirgazi areas (Konya-Central Anatolia). The investigated volcanic units are the southwestern part of the Neogene-Quaternary aged Cappadocia Volcanic Province (CVP) in Central Anatolia. Investigated volcanic rocks could be seperated into two subgroups (i) Karacadağ Volcanic Complex and (ii) Karapınar Volcanic Field (Gençoğlu Korkmaz et al 2022). Keller (1974) argues that the geological and genetic understanding of Karacadağ was hindered by the arrival of much younger basaltic scoria cones (Karapınar volcanics) that do not have a direct genetic relationship to the northeast of Karacadağ.

2. Geology and Volcanostratigraphy

Based on the previous study (Gençoğlu Korkmaz et al 2022) all geochemical (mineral and whole-rock), both radiogenic and stable isotope data, indicating that contamination played an important role during differentiation processes. All the data obtained suggest that the Karacadağ basaltic rocks stemmed from a subduction-modified lithospheric mantle source. On the other hand, the origin of the Karapınar basaltic rocks can be explained in terms of OIB-like melts contaminated with the Karacadağ volcanic rocks to gain an orogenic geochemical signature, which may be an alternative model for the origin of the CVP sodic alkali basalts (Gençoğlu Korkmaz et al 2022).

Volcanic stratigraphy is a fundamental component of geological mapping in volcanic areas as it yields the basic criteria and essential data for identifying the spatial and temporal relationships between volcanic products and intra/inter-eruptive processes. In such complex volcanic structures, it is almost impossible to create a single columnar section. Each cooling unit appears in different forms in different regions. For this reason, separate stratigraphic sections were created in 10 regions to create the volcanic stratigraphy. We can classify the KCVC as two different phases (Fig 1).

The lower volcanic phase of the Karacadağ Volcanic Complex are composed of andesitic-dacitic lava flows/domes and their pyroclastics. The products of this unit are generally massive and blocky. The thickness of the lava flows and pyroclastic products varies in the stratovolcano flanks. Generally, the volcanoclastics (block flow, volcanic breccia) are interbedded with the lava flows. We suggest the centre of the gaint andesitic-dacitic lava flows is probably Ovacık Crater ($R>3,5$ km). At the lower part of this phase, lahars are observed. The mineralogical composition and textural characteristics of the andesitic volcanics are different from each other in the lower phase. Some andesites include a variety type of enclaves. Also, the distribution of andesites showing marble cake texture is limited in the region. However, the upper volcanic phases contain mainly lava flows with the basaltic, aphyric-andesitic and trachytic composition and rarely pyroclastics products. These volcanics show flow banding texture and platy jointing. The rocks from the upper phase having trachytic texture under the microscope. Andesite-basaltic andesite and basaltic trachy-andesite lavas form the most common lava unit in the upper phase and overlie the pyroclastic succession. The youngest member of the volcanic association is represented by trachytic lavas which overlaid the basaltic lavas and associated pyroclastics in the Taşbudak area. At the lower parts of the upper volcanic units, massive and badly graded

volcanoclastics (volcanic breccia, ash flow) that overlies the widespread very thinly-bedded epiclastics are observed.

3. Material and Method

Zircon crystals from Andesite-1 were separated and embedded in epoxy resin in Dokuz Eylül University. The U-Pb LA-ICP-MS analyses were performed at the Dipartimento di Fisica e Geologia, Università di Perugia using an iCAPQ Thermo Fisher Scientific, quadrupole-based, ICP-MS coupled to a G2 Teledyne Photon Machine ArF (193 nm) LA system (2018). Uranium-Pb zircon analyses were calibrated with the international reference material zircon 91500 using a spot size of 25 µm and the Plešovice zircon had been used as quality control (Sláma et al., 2008).

4. Results

4.1. Stratigraphic Sections

Measured stratigraphic sections from the Karapınar-Karacadağ area demonstrate that the Mio-Pliocene aged lava flows exhibit that stratigraphic order (i) amphibole-bearing basaltic andesite, andesite, dacite at the lower stages; (Lower cooling phase) (ii) olivine bearing andesite at the middle, and biotite-amphibole bearing andesite and clinopyroxene-bearing basaltic andesite at the middle to upper parts (Lower cooling phase), (iii) clinopyroxene-orthopyroxene bearing basaltic andesite, glassy andesite, olivine bearing vesicular basalt at the middle to upper parts (Lower cooling phase), (iv) trachyte, trachyandesite, trachybasalt dikes, plugs and stocks at the top of the sections (Upper cooling phase). Quaternary volcanism overlies the trachytic-trachy basaltic units (from the upper phase), and the pyroclastics (from the lower phase) in the Gözbaşı-Meşeli area in the region. Measured stratigraphic sections from the Karapınar-Meke-Andıkları areas demonstrate that the Quaternary aged lava flows exhibit that stratigraphic order (i) Altered basaltic-andesitic, andesitic lava flows from previous phases, (ii) Calc-alkaline basaltic-basaltic andesitic-andesitic lava, ol+cpx basalt, cpx dominated andesite (iii) Scoria fall deposits (iv) mildly alkaline-calc-alkaline olivine rich basaltic lava flows, (v) calc-alkaline cpx+pl+q+ bearing basaltic, basaltic-andesitic, andesitic lava flows, well-graded base surges (vi) olivine-rare, cpx-bearing scoria fall deposits at the top of the sections (vii) welded scoria-agglutinate at the top of the Meke scoria cone.

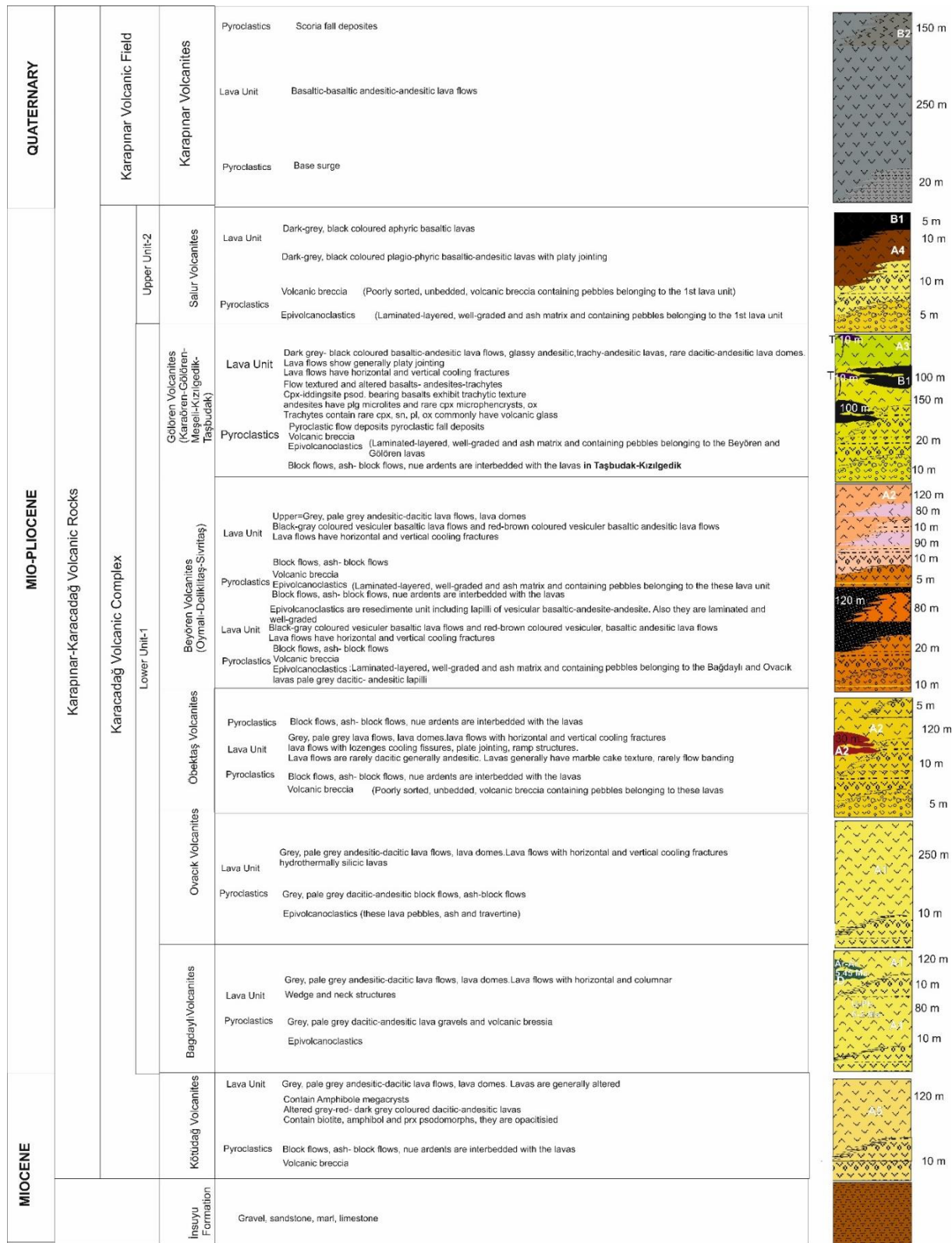


Figure 1. General stratigraphic section based on the ten different regions in the investigated area.

4.2. U-Pb ages

U-Pb geochronology yielded 1.84 ± 0.12 (Ma) crystallization ages from Zircon grains ($n=39$) within the Karacadağ Andesite (Fig 2-3) (biotite-amphibole bearing andesite; Andesite-1 from Gençoğlu Korkmaz et al 2022).

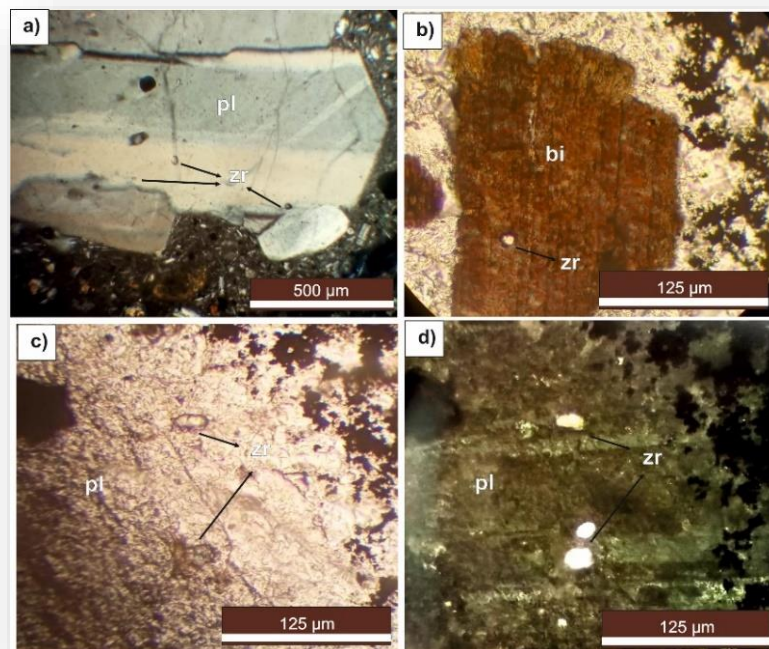


Figure 2. Zircon grains from the andesites.

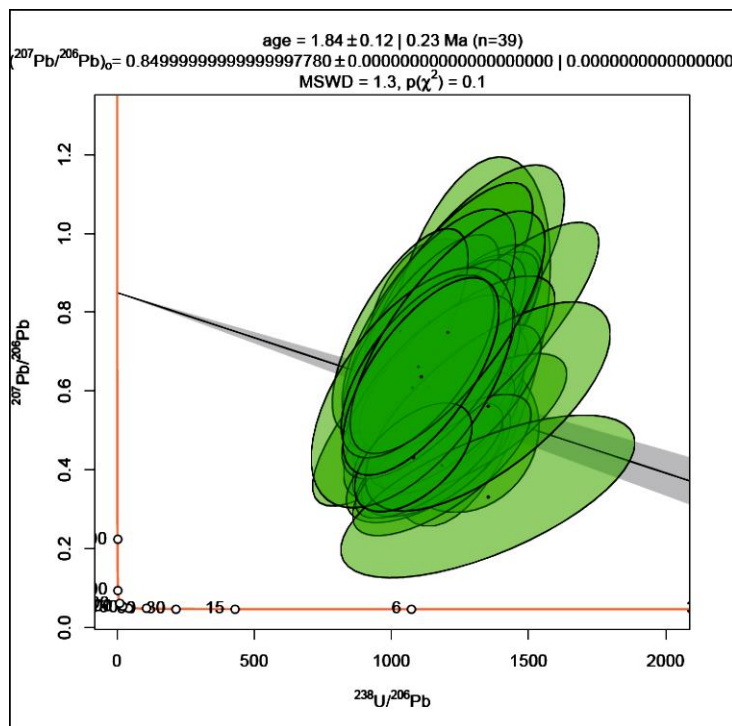


Figure 3. U-Pb concordia diagram of the Zircon grains within the Karacadağ andesites (andesite-1).

5. Conclusions

Petrographic investigations indicate that, all lava samples display several textures reflecting disequilibrium crystallization such as sieve texture in plagioclases and in some clino/orthopyroxenes, clinopyroxene crystals mantled by hornblende and reaction textures/rims in hornblend and biotite. These petrographic evidences suggest that magma replenishment processes (magma mixing/mingling, self/cryptic mixing) have a key role during the evolution of the Karacadağ Volcanic Complex and Karapınar Volcanic Field. Moreover, based on the geochronological data we claim that U-Pb zircon ages are more younger than Ar-Ar ages.

Acknowledgements: This work is part of the first author's PhD thesis in Karapınar-Emırgazi-Karacadağ area.

REFERENCES

- Ercan, T., Fujitami, T., Matsuda, J., Tokel, S., & Notsu, K. (1990). Hasandagi-Karacadag (Orta Anadolu) dolaylarındaki Senozoyik yaslı volkanizmanın kökeni ve evrimi. *Jeomorfoloji Dergisi*, 18, 39-54.
- Gençoğlu Korkmaz, G., Kurt, H., Asan, K., & Leybourne, M. (2022). Ar-Ar Geochronology and Sr-Nd-Pb-O Isotopic Systematics of the Post-collisional Volcanic Rocks from the Karapınar-Karacadağ Area (Central Anatolia, Turkey): An Alternative Model for Orogenic Geochemical Signature in Sodic Alkali Basalts. *Journal of Geosciences*, 67(1), 53-69.
- Gençoğlu Korkmaz, G., & Kurt, H. (2021). Interpretation of the Magma Chamber Processes with the help of Textural Stratigraphy of the Plagioclases (Konya-Central Anatolia). *Avrupa Bilim ve Teknoloji Dergisi* (25), 222-237.
- Gençoğlu Korkmaz, G., Kurt, H., & Asan, K. (2021). Classification and Generation of the Enclaves in Karapınar-Karacadağ Volcanic Rocks (Central Anatolia). *Turkish Journal of Geosciences*, 30-46. doi:10.48053/turkgeo.1018063.
- Gençoğlu Korkmaz, G., Kurt, H., Asan, K., & Kadıoğlu, Y. (2018). The first mineralogical and petrographical investigations of enclaves and their host rocks from the Karapınar-Karacadağ area (SE Konya, Turkey). Paper presented at the 36th National and the 3rd International Geosciences Congress.
- Keller, J. (1974). Quaternary Maar Volcanism near Karapınar in Central Anatolia. Symposium on Volcanism and Associated Metallogenesis, Bucharest., 19.
- Reid, M. R., Schleiffarth, W. K., Cosca, M. A., Delph, J. R., Blichert-Toft, J., & Cooper, K. M. (2017). Shallow melting of MORB-like mantle under hot continental lithosphere, Central Anatolia. *Geochemistry, Geophysics, Geosystems*, 18(5), 1866-1888. doi:10.1002/2016gc006772.
- Uslular, G., & Gençalioğlu-Kuşcu, G. (2019). Mantle source heterogeneity in monogenetic basaltic systems: A case study of Eğrikuyu monogenetic field (Central Anatolia, Turkey). *Geosphere*, 15(2), 29. doi:10.1130/ges01682.1.



Chairmen: Prof. Dr. Fetullah ARIK & Prof. Dr. Kürşad ASAN

Honorary speaker: Prof. Dr. Axel K. SCHMITT

Convenor: Dr. Gülin GENÇOĞLU KORKMAZ

Editor: Dr. Gülin GENÇOĞLU KORKMAZ (Geological Engineering Department -Konya Technical University)

Location: Konya Technical University, Geological Engineering Department, Konya/TURKEY (12-13 May 2022)



City of Konya and Mevlâna Museum



EBOOK ISBN : 978-605-74442-7-1

**Location: Konya Technical University,
Geological Engineering Department,
Konya/TURKEY**